Identification of a potent and selective σ₁ receptor agonist potentiating NGF-induced neurite outgrowth in PC12 cells

Daniela Rossi [a], Alice Pedrali [a], Mariangela Urbano [a], Raffaella Gaggeri [a], Massimo Serra [a], Leyden Fernández [b], Michael Fernández [c], Julio Caballero [d], Simone Ronsisvalle [e], Orazio Prezzavento [e], Dirk Schepmann [f], Bernhard Wuensch [f], Marco Peviani [g], Daniela Curti [g], Ornella Azzolina [a], Simona Collina [a,*]

[a] Department of Drug Sciences, University of Pavia, Viale Taramelli 12, 27100 Pavia, Italy
[b] Life Sciences, Computational Genomics Department, Barcelona Supercomputing Center, 08034 Barcelona, Spain
[c] Department of Bioscience and Bioinformatics, Kyushu Institute of Technology (KIT), 680-4 Kawazu, 820-8502 Iizuka, Japan
[d] Centro de Bioinformática y Simulación Molecular, Facultad de Ingeniería en Bioinformática, Universidad de Talca, 2 Norte 685, 721 Casilla, Talca, Chile
[e] Department of Drug Sciences, University of Catania, Viale A. Doria 6, 95125 Catania, Italy
[f] Institute of Pharmaceutical and Medicinal Chemistry, University of Muenster, Hittorfstrasse 58-62, 48149 Muenster, Germany
[g] Department of Legal Medicine, Forensic and Pharmaco-toxicological Sciences, Lab. of Cellular and Molecular Neuropharmacology, University of Pavia, Via Ferrata 9, 27100 Pavia, Italy

ABSTRACT

Herein we report the synthesis, drug-likeness evaluation, and in vitro studies of new sigma (σ) ligands based on arylalkenylaminic scaffold. For the most active olefin the corresponding arylalkylamine was studied. Novel arylalkenylamines generally possess high σ₁ receptor affinity (K_i values <25 nM) and good σ_1/σ_2 selectivity ($K_i\sigma_2$ >100). Particularly, the piperidine derivative (*E*)-**17** and its arylalkylamine analog (*R,S*)-**33** were observed to be excellent σ₁ receptor ligands (K_i = 0.70 and 0.86 nM, respectively) and to display significantly high selectivity over σ₂, μ-, and κ-opioid receptors and phencyclidine (PCP) binding site of the *N*-methyl-D-aspartate (NMDA) receptors. Moreover in PC12 cells (*R,S*)-**33** promoted the nerve growth factor (NGF)-induced neurite outgrowth and elongation. Co-administration of the selective σ₁ receptor antagonist BD-1063 totally counteracted this effect, confirming that σ₁ receptors are involved in the (*R,S*)-**33** modulation of the NGF effect in PC12 cells and suggesting a σ₁ agonist profile. As a part of our work, a three-dimensional σ₁ pharmacophore model was also developed employing GALAHAD methodology. Only active compounds were used for deriving this model. The model included two hydrophobes and a positive nitrogen as relevant features and it was able to discriminate between molecules with and without affinity toward σ₁ receptor subtype.

© 2011 Elsevier Ltd. All rights reserved.

1. Introduction

The sigma (σ) receptor is unique non-opioid, non-phencyclidine (PCP) binding site. To date, two subtypes of the σ receptor have been identified, the σ₁ and the σ₂. Concerning the σ₂ subtype, although it has not yet been cloned, accumulating evidences suggest the specific involvement of the receptor in the death signaling of cancer cells.[1,2] As regards to the σ₁ subtype, the receptor is ubiquitously expressed in mammalian tissues;[3] moreover it has been purified and cloned from several mammalian species as a 223 amino acid protein with 90% identical amino acid sequences across species.[4–7] The macromolecule contains three hydrophobic domains. Two of them are transmembrane-spanning helices with an extracellular loop in between and an intracellular C terminus.[8] The σ₁ is an intracellular receptor specifically localized in the

endoplasmic reticulum (ER) at the ER–mitochondria interface,[9] where it regulates ER–mitochondrion signaling and ER–nucleus crosstalk.[10] The receptor is considered to be an ER chaperone protein acting as inter-organelle signaling modulator because it can translocate to the plasma membrane or to other subcellular compartments under stressful conditions and/or pharmacological manipulation.[11,12] The most prominent action of σ₁ receptor is the modulation of voltage-regulated and ligand-gated ion channels, including Ca^{2+}, K^+, Na^+, Cl^-, and NMDA and IP3 receptors.[10] Moreover the σ₁ receptor can interact with ER-resident chaperones like Binding immunoglobulin Protein/78 kDa Glucose-Regulated Protein (BiP/GRP78), acting as sensor of ER-stress caused by unfolded proteins overload,[13] and it can promote cell survival by modulating the expression of B-cell lymphoma 2 (Bcl-2), the major antiapoptotic member of the Bcl-2 family.[14] Literature evidences suggest the involvement of the receptor in diseases such as drug addiction, depression, neurodegeneration, pain-related disorders, and cancer.[1] Recently, a mutation in the σ₁ receptor gene was

* Corresponding author. Tel.: +39 0382987379; fax: +39 0382422975.
  E-mail address: simona.collina@unipv.it (S. Collina).

found to be associated with frontotemporal lobar degeneration (FTLD), the most common cause of dementia under the age of 65 years.[15] Interestingly, the σ_1 receptor has been found implicated in neurite sprouting in vitro suggesting a role for the receptor in neuroplasticity. In fact, experiments on PC12 cells, an in vitro model of neuronal differentiation,[16] have shown that overexpression of σ_1 receptor or exposure to σ_1 receptor agonists potentiate neurite outgrowth and elongation induced by growth factors, such as nerve growth factor (NGF) or epidermal growth factor (EGF).[17,18] In line, experiments performed on organotypic spinal cord cultures have highlighted that exposure to a σ_1 receptor agonist protects motoneurons against glutamate-induced excitotoxicity and increases neurite elongation.[19]

Therefore, the identification of new and potent ligands, with high selectivity for the σ_1 receptor and defined action, will be of great interest to better understand the role of σ_1 receptor in different pathologies. This may pave the way to development of innovative therapeutic strategies addressed to modulate neuronal protection, plasticity, and regeneration.

In the last 10 years our research group has conducted extensive studies aimed at discovering novel σ ligands potentially useful in neurodegenerative diseases treatment. In this context, we reported the design, synthesis and biological evaluation of various σ_1 receptor ligands based on both arylalkenyl- and arylalkylaminic scaffolds (Fig. 1).[20] In that paper we carefully evaluated the influence of different aromatic portions (naphth-2-yl, naphth-1-yl, biphen-4-yl, 6-hydroxy-, and 6-methoxy-naphth-2-yl) combined with two aminic moieties (N,N-dimethylamine and N-benzyl-N-methylamine) on σ receptors affinity and selectivity. We also studied the influence of the three carbon spacer between the aromatic portion and the aminic moiety on σ receptor binding by preparing new derivatives characterized by olefinic, alkylic and alcoholic spacers (arylalkenyl-, arylalkylamines, and arylalkylaminoalcohols, respectively, Fig. 1).[21]

In the present contribution we extended our SAR studies further with arylalkenylamines structurally related to (E)-1–4 (Fig. 2);[20] particularly, herein we report the synthesis, drug-likeness evaluation, and in vitro profile of new derivatives. For the most active olefin, the corresponding arylalkylamine was studied. Moreover, we report on a deep investigation of the pharmacological profile of the most promising compounds by evaluating their effect on NGF-induced neurite outgrowth and elongation in PC12 cells.

Finally, we report on the development of a σ_1 pharmacophore model based on arylalkenyl- and arylalkylamines using GALAHAD (Genetic Algorithm with Linear Assignment of Hypermolecular Alignment of Datasets),[22] with the final aim of obtaining a model that could provide a rational hypothetical picture of the chemical features responsible for the σ_1 affinity of these compounds.

2. Results

2.1. Chemistry

At first the synthesis of β-aminoketones **5–7** was accomplished via the Michael addition of N,N-dimethylamine, N-benzyl-N-methylamine, and piperidine to but-3-en-2-one, essentially according to the methodologies already described by us (Scheme 1).[20,21] Similarly, the Michael addition of both 4-benzylpiperidine
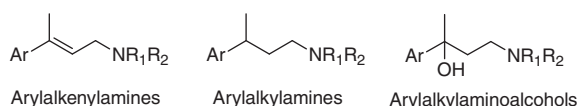

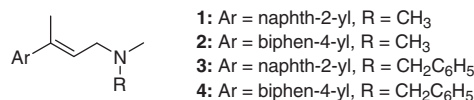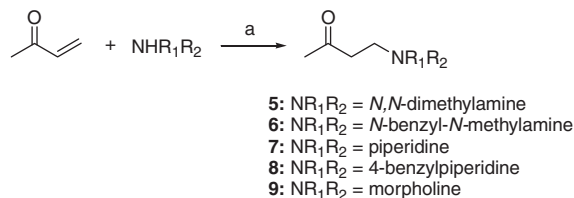**Figure 1.** General structures of arylalkenyl-, arylalkylamines, and arylalkylaminoalcohols.
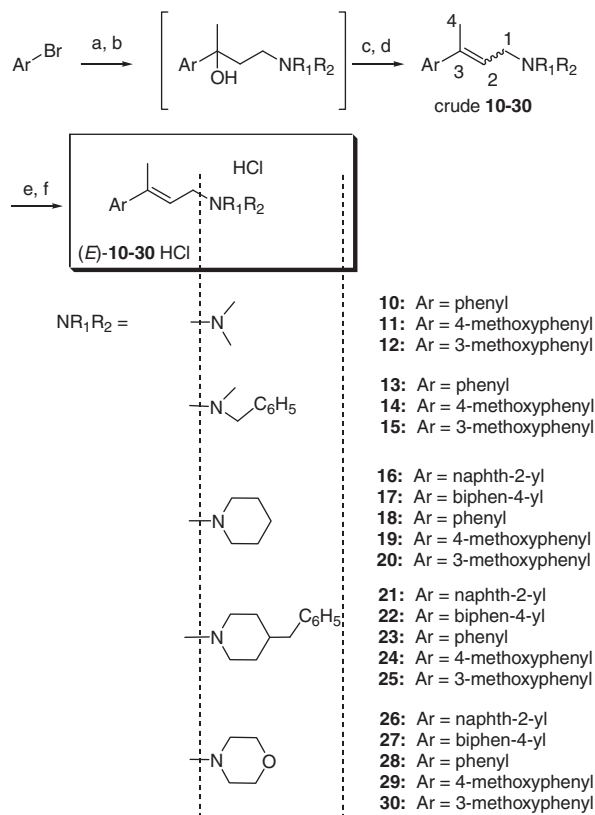

1: Ar = naphth-2-yl, R = CH$_3$
2: Ar = biphen-4-yl, R = CH$_3$
3: Ar = naphth-2-yl, R = CH$_2$C$_6$H$_5$
4: Ar = biphen-4-yl, R = CH$_2$C$_6$H$_5$

Figure 2. Structure of arylalkenylamines (E)-**1–4**.

5: NR$_1$R$_2$ = N,N-dimethylamine
6: NR$_1$R$_2$ = N-benzyl-N-methylamine
7: NR$_1$R$_2$ = piperidine
8: NR$_1$R$_2$ = 4-benzylpiperidine
9: NR$_1$R$_2$ = morpholine

Scheme 1. Synthesis of β-aminoketones **5–9**. Reagents and conditions: (a) anhydrous toluene, reflux for compounds **5**, **6**; PEG 400, rt for compounds **7–9**.

and morpholine to but-3-en-2-one in polyethylene glycol 400 (PEG 400) afforded β-aminoketones **8** and **9**, respectively (Scheme 1). After an acid–base work up, pure **9** was obtained in good yields; concerning compound **8,** a further purification by filtration on an alumina pad was required.

The synthesis of arylalkenylamines **10–30** was then carried out via the nucleophilic addition of the opportune aromatic anion to β-aminoketones **5–9**, followed by direct dehydration under standard acidic conditions (37% HCl, Scheme 2, method I, see experimental section).[20] A basic work-up allowed the isolation of the desired olefinic compounds as free bases. The reaction resulted highly regio- and stereoselective for all arylalkenylamines, as confirmed by ^{1}H NMR analysis and NOESY experiments of crude compounds, in accordance with our previous experience.[20]

10: Ar = phenyl
11: Ar = 4-methoxyphenyl
12: Ar = 3-methoxyphenyl

13: Ar = phenyl
14: Ar = 4-methoxyphenyl
15: Ar = 3-methoxyphenyl

16: Ar = naphth-2-yl
17: Ar = biphen-4-yl
18: Ar = phenyl
19: Ar = 4-methoxyphenyl
20: Ar = 3-methoxyphenyl

21: Ar = naphth-2-yl
22: Ar = biphen-4-yl
23: Ar = phenyl
24: Ar = 4-methoxyphenyl
25: Ar = 3-methoxyphenyl

26: Ar = naphth-2-yl
27: Ar = biphen-4-yl
28: Ar = phenyl
29: Ar = 4-methoxyphenyl
30: Ar = 3-methoxyphenyl

Scheme 2. Synthesis of arylalkenylamines (E)-**10–30** HCl (method I). Reagents and conditions: (a) t-BuLi, anhydrous Et$_2$O, −78 °C to rt; (b) ketones **5–9**, −78 °C; (c) 37% HCl, rt; (d) 1 N NaOH; (e) 37% HCl, rt; (f) crystallization from acetone.

Arylalkenylamines **10–30**, after purification by either crystallization or flash chromatography (when required, see experimental section), were converted into the corresponding hydrochlorides and successively crystallized from acetone, yielding desired (E)-arylalkenylamines in satisfactory yields, with the only exception of **19** HCl and **29** HCl. In order to improve the reaction yields and to prepare compounds (E)-**19** and (E)-**29** in amount suitable for biological investigation, we changed our synthetic strategy. Thus, racemic arylalkylaminoalcohols **31** and **32** were synthesized via nucleophilic addition of the appropriate arylic anion to the opportune β-aminoketone and isolated in good yields after an acid–base work up; arylalkenylamines **19** and **29** were then prepared by regioselective dehydration of the respective arylalkylaminoalcohols employing the polymer-bound triphenylphosphine (TPPP)-iodine system (Scheme 3).[21] Dehydration reaction of alcoholic intermediates resulted stereoselective: the main reaction product was the (E) isomer for both substrates tested, as confirmed by both ^{1}H NMR analysis of crude products and NOE experiments.[21] Crude **19**, **29** were then converted into the corresponding hydrochlorides and crystallized from acetone, providing pure (E)-**19** HCl and (E)-**29** HCl in satisfactory yields.

Finally, (R,S)-**33** HCl was synthesized by catalytic reduction of the corresponding arylalkenylamine (E)-**17** in hydrogen atmosphere, using Pd(0) EnCat™ 30NP as catalyst (Scheme 4),[21] easily isolated by solid phase extraction (SPE, SCX cartridge) and then converted into the corresponding hydrochloride.

2.2. Biology

2.2.1. Receptor binding studies

The binding properties of arylalkenylamines (E)-**10–30** HCl were investigated for σ receptor subtypes (σ$_1$ and σ$_2$) expressed in guinea pig brain membranes. [^{3}H]-(+)-pentazocine (3 nM) was employed for σ$_1$ receptor binding assays in the presence of haloperidol (10 μM) to measure the nonspecific binding. The non selective radioligand [^{3}H]-1,3-di-o-tolylguanidine ([^{3}H]-DTG, 3 nM) was employed for σ$_2$ receptor binding studies in the presence of an excess of [2S-(2α,6α,11R)]-1,2,3,4,5,6-hexahydro-6,11-dimethyl-3-(2-propenyl)-2,6-methano-3-benzazocin-8-ol [(+)-SKF10,047, 0.4 μM] and non-tritiated DTG (5 μM) to mask σ$_1$ receptors and

to define nonspecific binding, respectively. The σ receptor binding affinities, expressed as inhibition constants (K$_i$), are summarized in Table 1.

The binding properties of (E)-**10–30** HCl were investigated also for μ-, κ-opioid receptors and PCP binding site of NMDA receptors using, as receptor material, guinea pig brain and pig brain cortex, respectively. [^{3}H][D-Ala[2],Me-Phe[4],Gly-ol[5]]enkephalin ([^{3}H]-DAMGO, 1 nM, μ), [^{3}H]-(5R,7R,8β-(−)-N-methyl-N-[7-(1-pyrrolidinyl)-1-oxaspiro (4–5) dec-8-yl]-benzeneacetamide) ([^{3}H]-U 69,593, 1 nM, κ) and [^{3}H]-(5R,10S)-(+)-5-methyl-10,11-dihydro-5I-dibenzo-[α,β]cyclohepten-5,10-imine ([^{3}H]-MK-801, 2 nM, NMDA) were employed as specific radioligands. The non-specific binding was determined with unlabeled naloxone (10 μM, μ), unlabeled U 69,593 (10 μM, κ) and unlabeled (+)-MK-801 (10 μM, PCP binding site of NMDA). The residual binding of the radioligand is given at a concentration of 1 μM (μ and κ receptor binding assays) or 10 μM (NMDA receptor binding assays) of tested compounds. When a significant inhibition of the radioligand was observed, the K$_i$ value was determined. Results are summarized in Table 1.

2.2.2. NGF-induced neurite outgrowth in PC12 cells

In a preliminary set of experiments, we assessed the effect of a known σ$_1$ agonist, 2-(4-morpholinethyl)1-phenylcyclohexanecarboxylate hydrochloride (PRE-084), and an antagonist, 1-[2-(3,4-dichlorophenyl)ethyl]-4-methylpiperazine dihydrochloride (BD-1063), on NGF-induced neurite outgrowth in PC12 cell line. Cells were treated with NGF (2.5 ng/mL) alone or in the presence of PRE-084 or BD-1063 for 5 days. NGF alone promoted neurite sprouting in 18.1% ± 1.0 of the PC12 cells in culture (n = 8 different experiments); the average neurite length was 100.3 ± 5.0 μm. PRE-084 (10 μm) significantly increased the percentage of cells with neurite outgrowth to 27.5% ± 1.5 (p <0.01) (Fig. 3A) and the length of neurites to 181.3 ± 11.7 μm (p <0.01) (Fig. 3B), whereas it was ineffective at 2.5 μM (Fig. 3). BD-1063 (5 μM), co-administered with PRE-084, totally counteracted the effect of PRE-084 on the percentage of cells with neurite outgrowth (16.0% ± 2.4, p <0.025) and significantly decreased the effect of PRE-084 on neurite elongation (140.1 ± 10.8 μm, corresponding to a 23% decrease of neurite length, p <0.025).

Compounds (E)-**17** HCl and (R,S)-**33** HCl were then tested in this experimental setting to characterize their pharmacological profile and to analyze their effect on NGF-induced neurite outgrowth. (R,S)-**33** HCl was able to increase the percentage of cells with neurite outgrowth starting from 0.01 μM (23.4% ± 1.8, p <0.05) (Fig. 4A), whereas at the same concentration no significant response was produced by PRE-084. (R,S)-**33** HCl also increased neurite elongation starting from 0.25 μM (130.9 ± 7.2 μm, p <0.01) (Fig. 4B). Co-administration of BD-1063 (5 μM) with the (R,S)-**33** HCl (0.25 μM), totally counteracted the effect of (R,S)-**33** HCl on neurite outgrowth (18.6 ± 1.0, p <0.05) and decreased neurite length of 31% (p <0.01) (data not shown).

(E)-**17** HCl, at the concentrations 0.05, 0.25, and 2.5 μM, did not significantly enhance NGF-induced neurite outgrowth or elongation (Fig. 5). Co-administration of (E)-**17** HCl (2.5 μM) with BD-1063 (5 μM) significantly decreased (p <0.05) the percentage of cells with neurite outgrowth.

2.3. Computational study

2.3.1. Drug-likeness studies

The 'drug-likeness' of the novel σ receptor ligands was assessed on the basis of their structural properties by applying the Lipinski's 'rule of five' (Table 2).[23] Concerning lipophilicity, both clogP and clogD values were calculated since, given their apparent pK$_a$ values, all molecules are present mainly in the protonated form at physiological pH (7.4). For all the compounds studied, none of
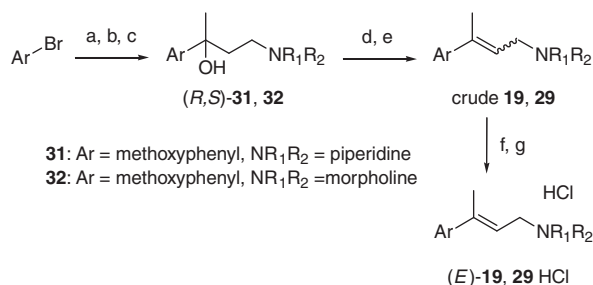
Scheme 3. Synthesis of arylalkenylamines (E)-**19**, **29** HCl (method II). Reagents and conditions: (a) t-BuLi, anhydrous Et$_2$O, −78 °C to rt; (b) ketones **7** or **9**, −78 °C; (c) H$_2$O, rt; (d) I$_2$, TPPP, rt; (e) aq 5% NaHSO$_3$, rt; (f) 37% HCl, rt; (g) crystallization from acetone.
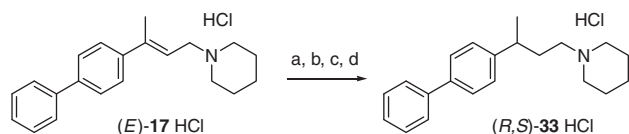
Scheme 4. Synthesis of arylalkylamine (R,S)-**33**. Reagents and conditions: (a) SCX cartridge; (b) H$_2$, Pd(0) EnCat™ 30NP, abs EtOH, rt; (c) SCX cartridge; (d) 37% HCl, rt.

Table 1
Affinities of compounds (*E*)-**1–4**, **10–30** HCl toward σ_1, σ_2, NMDA, μ-, and κ-opioid receptors

Compd	$K_i \pm SEM$ (nM)		σ_2/σ_1	Inhibition of the radioligand		
	σ_1[a]	σ_2[b]		μ-Opioid[c]	κ-Opioid[d]	NMDA[e]
(*E*)-**1** HCl[f]	19.8 ± 0.3	148 ± 4	7.5	NT[g]	NT	NT
(*E*)-**2** HCl[f]	1.40 ± 0.2	106 ± 6	75.7	NT	NT	NT
(*E*)-**3** HCl[f]	7.88 ± 0.3	873 ± 12	110.8	NT	NT	NT
(*E*)-**4** HCl[f]	6.32 ± 0.3	75.7 ± 4	12.0	NT	NT	NT
(*E*)-**10** HCl	>1000	>1000	—	0%	0%	0%
(*E*)-**11** HCl	806 ± 63	>1000	—	10%	20%	0%
(*E*)-**12** HCl	>1000	>1000	—	17%	5%	60%
(*E*)-**13** HCl	92.0 ± 12	61.0 ± 5	0.7	119[h]	438[h]	67%
(*E*)-**14** HCl	5.25 ± 1.0	155 ± 15	29.5	92[h]	197[h]	27%
(*E*)-**15** HCl	10.0 ± 1.8	163 ± 11	16.3	49%	301[h]	8%
(*E*)-**16** HCl	0.97 ± 0.3	35.1 ± 9	36.2	23%	44%	16%
(*E*)-**17** HCl	0.86 ± 0.4	111 ± 21	129.1	0%	6%	32%
(*E*)-**18** HCl	459 ± 21	191 ± 11	0.4	19%	0%	0%
(*E*)-**19** HCl	14.0 ± 3.0	149 ± 13	10.6	36%	14%	0%
(*E*)-**20** HCl	91.0 ± 11	294 ± 22	3.2	21%	22%	0%
(*E*)-**21** HCl	23.0 ± 2.6	16.0 ± 1.1	0.7	38%	10%	17%
(*E*)-**22** HCl	7.02 ± 0.9	18.0 ± 1.7	2.6	0%	10%	17%
(*E*)-**23** HCl	1.07 ± 0.3	5.49 ± 0.5	5.1	152[h]	189[h]	0%
(*E*)-**24** HCl	4.14 ± 0.3	7.10 ± 1.2	1.7	149[h]	157[h]	0%
(*E*)-**25** HCl	7.70 ± 1.0	5.80 ± 1.0	0.8	36%	214[h]	36%
(*E*)-**26** HCl	9.60 ± 1.6	229 ± 32	23.9	44%	15%	31%
(*E*)-**27** HCl	11.6 ± 2.0	386 ± 27	33.3	52%	10%	69%
(*E*)-**28** HCl	>1000	>1000	—	12%	3%	19%
(*E*)-**29** HCl	>1000	>1000	—	0%	8%	10%
(*E*)-**30** HCl	>1000	>1000	—	46%	10%	20%
(*R,S*)-**33** HCl	0.70 ± 0.3	103 ± 10	147.1	0%	36%	25%

Values are means ± SEM of three experiments.
[a] Displacement of 3 nM [³H]-(+)-pentazocine.
[b] Displacement of 3 nM [³H]-DTG.
[c] Displacement of 1 nM [³H]-DAMGO.
[d] Displacement of 1 nM [³H]-U 69593.
[e] Displacement of 2 nM [³H]-MK-801.
[f] For comparative purposes, affinity data were included.[16]
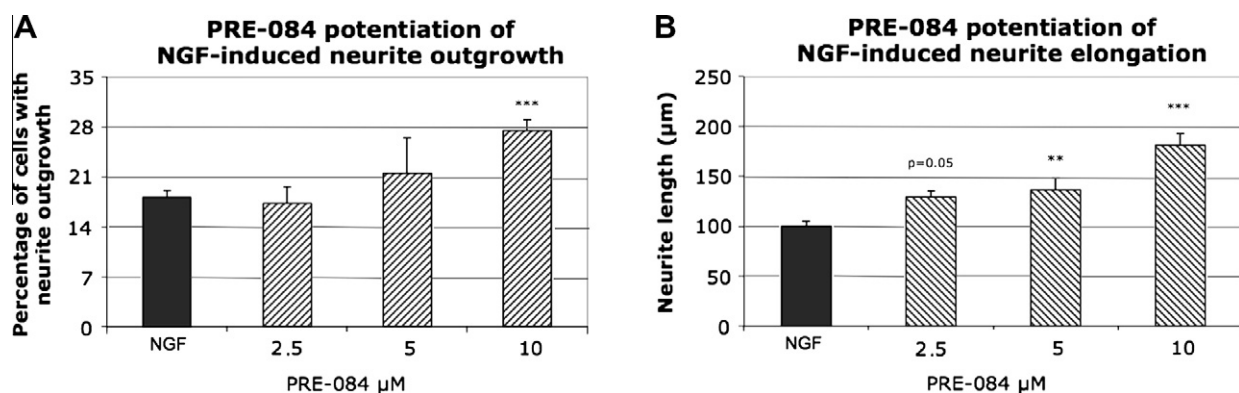[g] Not tested.
[h] K_i (nM).

Figure 3. Potentiating effect of σ_1 receptor agonist PRE-084 on NGF (2.5 ng/mL)-induced neurite (A) outgrowth and (B) elongation in PC12 cells. Histograms represent the mean ± SEM of at least three different experiments. **, $p < 0.025$; ***, $p < 0.01$ versus NGF alone.

the criteria was violated, with the only exception of **22** HCl which had a log*D* value above 5. Thus, compounds theoretically should have good absorption and/or permeability properties.

2.3.2. Pharmacophore modeling studies

A σ_1 pharmacophore model was developed by using GALAHAD (Genetic Algorithm with Linear Assignment of Hypermolecular Alignment of Datasets).[22] GALAHAD models were derived by using only ten active ligands as a training set [compounds **4**, **16**, **23–27**, **33** herein presented and the structurally related compounds **38** and **43** previously described by us (Fig. 6)].[20]

In detail, 20 pharmacophore models were retained after GALAHAD run using compounds of the training set. Each of the obtained models represents a different tradeoff among the conflicting demands of maximizing steric consensus (measured by steric overlap: SO), maximizing pharmacophore consensus (measured by pharmacophoric similarity: PhS), and minimizing energy (measured by strain energy: SE). All the obtained models were derived from more than seven ligands. In addition, they had Pareto rank 0; this means no one model is superior to any other. GALAHAD models were compared according to Pareto ranking. Small value of SE and high values of SO and PhS are desired for the best
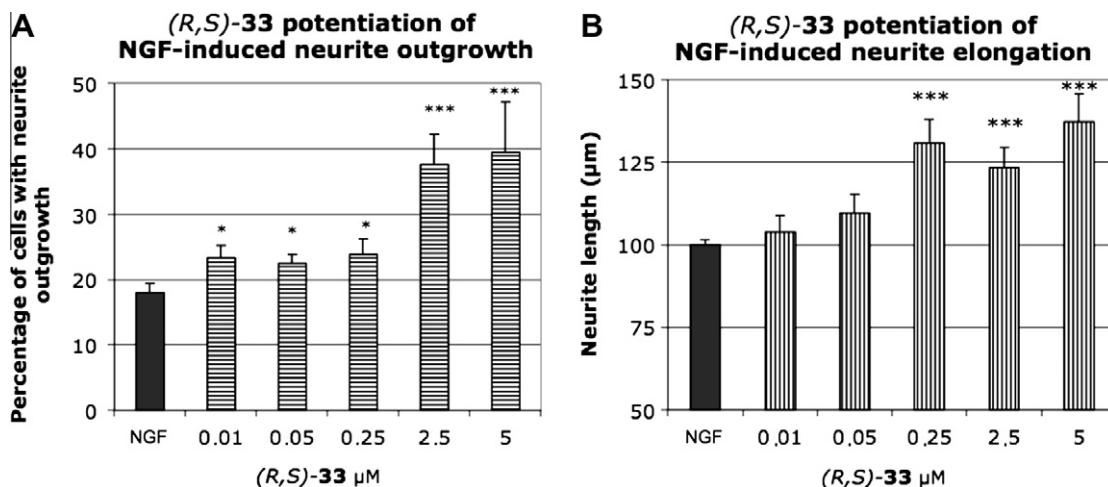
Figure 4. Potentiating effect of σ_1 receptor ligand (R,S)-**33** HCl on NGF (2.5 ng/mL)-induced (A) neurite outgrowth and (B) elongation in PC12 cells. Histograms represent the mean ± SEM of at least three different experiments. *, $p < 0.05$; ***, $p < 0.01$ versus NGF alone.
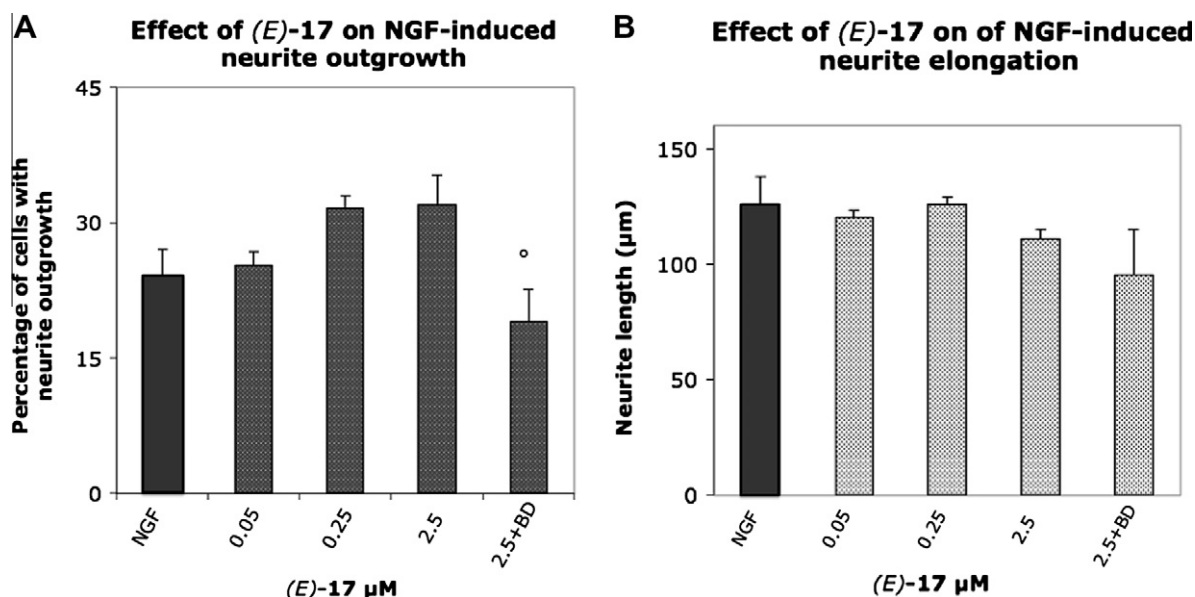

Figure 5. Effect of σ_1 receptor ligand (E)-**17** HCl on NGF (2.5 ng/mL)-induced neurite (A) outgrowth and (B) elongation in PC12 cells. Where indicated (BD), BD-1063 (5 µM) was co-administered with (E)-**17** HCl. °, $p < 0.05$ versus (E)-**17** HCl without BD-1063.

model. The higher value of SE between all the models is 45.44; and the lower value is 25.62. In general, SE values were closer to the maximum for the majority of models; models with low SE value had the lowest SO and PhS values. SO also had variation between the minimum (SO = 145.8) and the maximum (SO = 225.4) considering all the twenty models. Finally, PhS had variation between 19.5 (the minimum) and 30.5 (the maximum). With the intention to select the best model, we construct a 3D plot to visualize the Pareto surface as previously described by us.[24] The best GALAHAD model had SE = 39.96, SO = 202.4 and PhS = 26.9 (Fig. 7). It is comprised of all the 10 structures, one conformer for each molecule in the training set, plus a 3D database query derived from features more or less shared among them. All conformers aligned represent low-energy conformations of the molecules and it can be seen that the final alignment shows a satisfactory superimposition of the pharmacophoric points. In Figure 7, cyan and red spheres indicate hydrophobes and positive nitrogens, respectively. The best model includes 3 pharmacophore features: two hydrophobes (H1 and H2) and one positive nitrogen (N1). The positive nitrogen
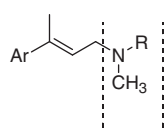
represented by N1 indicates that a positive charged atom is a requirement of σ_1 ligands. This feature seems to be a requirement of compounds to have affinity for σ_1 receptor; the two hydrophobic moieties of the pharmacophore schematically represented by H1 and H2 reflect the need for a hydrophobic structure as the skeleton of the σ_1 ligands with an angular disposition.

We evaluated how well the model reflects σ_1 binding affinity. For this, the best model was used as a template in aligning the full DS including compounds **1–29** and **33** herein presented and the structurally related compounds **34–44** previously described by us (Fig. 6).[20] We ran a partial least square (PLS) analysis by using the features of the model as molecular descriptors to predict the activities of all compounds. The scatter plot of the calculated versus experimental values of $\log(1/K_i)$ using the GALAHAD model is shown in Figure 8. The affinity $\log(1/K_i) = -1.4$ was selected as the threshold value between active and inactive compounds. According to this graph, the model was able to identify active compounds from the set of molecules which were not used in deriving the model. Fifteen molecules that do not participate in the

Table 2
Calculated druglike properties of compounds (E)-**10–30** HCl and (R,S)-**33** HCl

Compound	log P	log D[a]	pK_a	Rotatable bonds	H-Bond acceptors	Molecular weight
(E)-**10** HCl	2.82	1.50	8.70	3	1	175.27
(E)-**11** HCl	2.67	1.32	8.73	5	2	205.30
(E)-**12** HCl	2.67	1.36	8.68	5	2	205.30
(E)-**13** HCl	4.55	3.26	8.66	5	1	251.37
(E)-**14** HCl	4.39	3.08	8.69	7	2	281.39
(E)-**15** HCl	4.39	3.12	8.64	7	2	281.39
(E)-**16** HCl	4.66	3.07	8.98	3	1	265.39
(E)-**17** HCl	5.32	3.82	8.89	4	1	291.43
(E)-**18** HCl	3.67	2.12	8.94	3	1	215.33
(E)-**19** HCl	3.52	2.04	8.87	5	2	245.36
(E)-**20** HCl	3.52	2.08	8.82	5	2	245.36
(E)-**21** HCl	6.53	4.86	9.05	5	1	355.52
(E)-**22** HCl	7.19	5.60	8.97	6	1	381.55
(E)-**23** HCl	5.54	3.91	8.64	5	1	305.46
(E)-**24** HCl	5.38	3.82	8.95	7	2	335.48
(E)-**25** HCl	5.38	3.86	8.91	7	2	335.48
(E)-**26** HCl	3.59	3.49	6.78	3	2	267.37
(E)-**27** HCl	4.25	4.17	6.69	4	2	293.40
(E)-**28** HCl	2.61	2.51	6.74	3	2	217.31
(E)-**29** HCl	2.45	2.37	6.67	5	3	247.33
(E)-**30** HCl	2.45	2.37	6.67	5	3	247.33
(R,S)-**33** HCl	5.43	3.00	9.87	5	1	293.45

[a] Determined at pH 7.4.
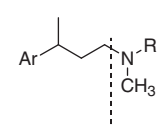
Figure 6. Chemical structure and σ_1 binding affinity data of compounds **34–44**.

generation of the model have $\log(1/K_i)$ values above -1.4 (Fig. 8). From them, 40% of the active molecules were correctly predicted. On the other hand, 12 molecules that do not participate in the generation of the model, have $\log(1/K_i)$ values below -1.4; none was predicted with an activity greater than this value.

3. Discussion

The arylalkenylamines herein presented generally showed interesting binding properties for σ_1 receptor subtype (K_i values <25 nM, Table 1). As evidenced in Figure 9A, all the 4-benzyl-piperidine derivatives (E)-**21–25** HCl revealed high affinity for σ_1 receptor subtype, independently of the aromatic moiety of the molecule (K_i values ranging from 1.07 nM to 23.0 nM). On the contrary, a dramatic decrease in σ_1 receptor affinity was generally evidenced for morpholine derivatives [$K_i\sigma_1$ >1000 nM], with the only excep-

tion of the naphth-2-yl derivative (E)-**26** HCl and the biphen-4-yl derivative (E)-**27** HCl, which interact in the low nanomolar range with the σ_1 receptor subtype (K_i = 9.60 ± 1.6 nM and 11.6 ± 2.0 nM, respectively). An analogous trend was observed for the N,N-dimethylamine compound series: only the naphth-2-yl derivative (E)-**1** HCl and the biphen-4-yl derivative (E)-**2** HCl significantly interact with σ_1 receptor subtype (K_i = 19.8 ± 0.3 and 1.40 ± 0.2 nM, respectively). Concerning σ_2 receptor affinity, only the 4-benzyl-piperidine derivatives (E)-**21–25** HCl revealed an interesting affinity for σ_2 receptor subtype, having K_i values ranging from 5.49 to 18.0 nM (Fig. 9B).

Biological results discussed so far clearly evidenced that the arylalkenylamines considered in this study generally possess high σ_1 receptor affinity and good σ_1/σ_2 selectivity, with the only exception of (E)-**21–25** HCl, for which good binding affinity for both σ receptor subtypes was proved. Therefore, they could represent a useful starting point for the next development of σ ligands potentially helpful in tumor diagnosis.[25]

Among the considered arylalkenylamines, the most interesting one in terms of both σ_1 receptor affinity and selectivity over σ_2 receptor subtype is the biphen-4-yl derivative (E)-**17** HCl (K_i = 0.86 ± 0.4 nM, $K_i\sigma_2/K_i\sigma_1$ = 129.1), bearing the piperidine nucleus as aminic moiety. Thus we prepared the corresponding arylalkylamine derivative (R,S)-**33** HCl: similar σ_1 receptor affinity and σ_1/σ_2 selectivity were observed (K_i = 0.70 ± 0.3 nM, $K_i\sigma_2/K_i\sigma_1$ = 147.1).

In order to widen the binding profile of newly synthesized compounds, their affinity toward µ- and κ-opioid receptors and PCP binding site of the NMDA receptors was also investigated (Table 1). With regard to µ- and κ-opioid receptor binding, novel compounds generally showed low affinity for both receptor subtypes, with the only exception of (E)-**13, 14** HCl and (E)-**23, 24** HCl (K_i values between 92 and 152 nM at µ-opioid receptors and between 157 and 438 nM at κ-opioid receptors). Compounds (E)-**15** HCl and (E)-**25** HCl showed a moderate inhibition of the radioligand only in the κ-opioid receptor binding assays (K_i = 301 and 214 nM, respectively). Concerning binding studies at the PCP binding site of the NMDA receptors, none of the tested compounds displayed a significant binding affinity. Only compounds (E)-**12, 13** HCl, and (E)-**27** HCl caused an inhibition of the radioligand higher then 50% at the screening concentration of 10 µM.
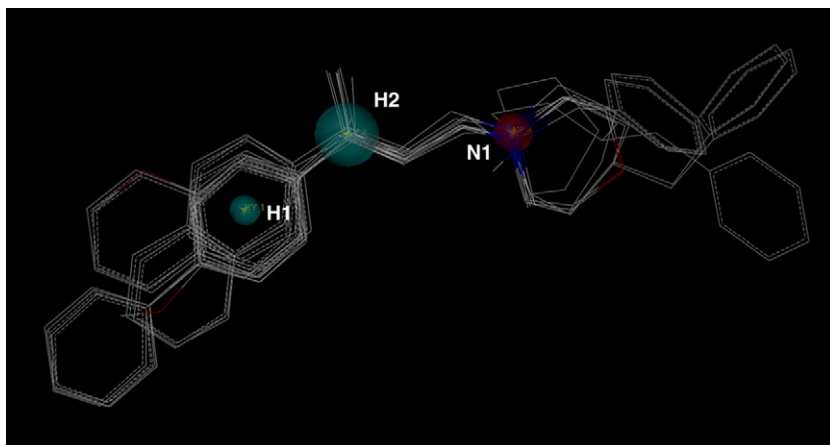
Figure 7. Selected pharmacophore model and molecular alignment of the compounds used to elaborate the model. Cyan and red spheres are represented for hydrophobes and positive nitrogens, respectively.
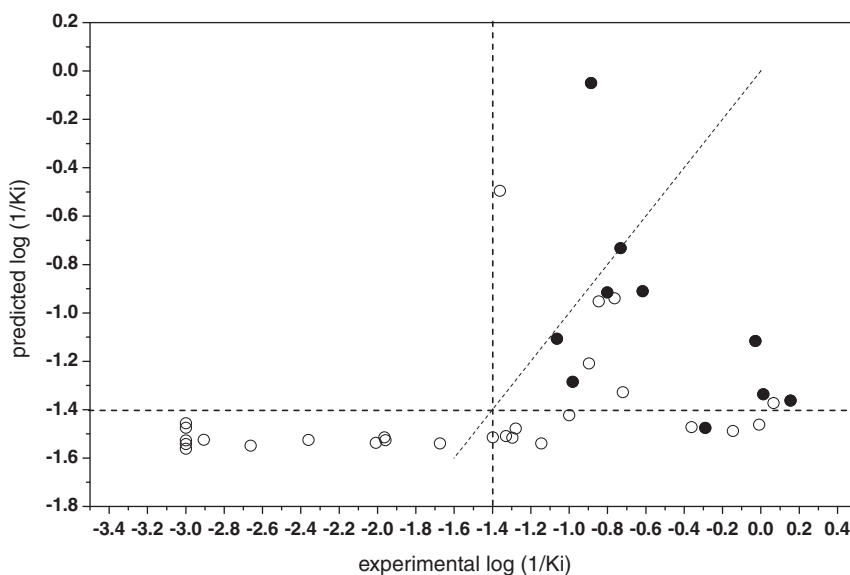

Figure 8. Scatter plot of the experimental activities versus predicted activities for pharmacophore model (●) predictions for compounds used to elaborate the model (○) predictions for the remaining compounds. The line in $\log(1/K_i) = -1.4$ means that this value was selected as the threshold value between active and inactive compounds.

Overall binding results confirmed that (E)-**17** HCl and (R,S)-**33** HCl are the most promising σ_1 ligands of this study, displaying high selectivity toward σ_2, μ-, and κ-opioid receptors and PCP binding site of the NMDA receptors. Moreover, these compounds theoretically should have good permeability properties and should effectively permeate the brain blood barrier, having $\log P$ values higher then 2, as evidenced by drug likeness studies.

Thus, (E)-**17** HCl and (R,S)-**33** HCl have been selected by us for a deeper evaluation of their biological profile. In this contest, the NGF induced-PC12 cells neurite outgrowth and elongation model represents a valuable tool for drawing agonist/antagonist profile of selected compounds. Indeed, it has been reported that σ_1 agonists potentiate the effect of NGF in PC12 cells,[17] while σ_1 receptor antagonists do not exert any relevant influence on this NGF-induced effect. Particularly, fluvoxamine, 1-[2-(3,4-dimethoxyphenyl)ethyl]-4-(3-phenylpropyl)piperazine (SA4503), 4-phenyl-1-(4-phenylbutyl) piperi-dine (PPBP), dehydroepian-drosterone (DHEA)-sulfate[26], and donezepil[27] significantly increase the percentage of cells with NGF-induced neurite outgrowth in the concentration range of 0.1–10 µM. This effect is counteracted by co-administration of selective σ_1 receptor antagonists. Further-

more, cells treatment with SA4503 (1.0 µM) or fluvoxamine (10 µM) also potentiates NGF-induced neurite elongation.[26]

To validate this assay, we firstly performed preliminary experiments treating PC12 cells with NGF and with the well known σ_1 receptor ligands PRE-084 and BD-1063, having agonist and antagonist profile, respectively. In agreement with literature results, NGF promoted neurite sprouting as well as neurite elongation. The well characterized σ_1 receptor agonist PRE-084 significantly increased the percentage of cells with neurite outgrowth and length of neurites only at the concentration of 10 µM (Fig. 3). Moreover, the σ_1 receptor antagonist BD-1063 (5 µM), when co-administered with PRE-084, totally counteracted the effect of the agonist on both neurite outgrowth and elongation.

Concerning our molecules, compound to be highlighted is (R,S)-**33** HCl: it was effective in increasing both neurite outgrowth and elongation at lower concentration with respect to PRE-084 (0.01 µM vs 10 µM for neurite outgrowth and 0.25 µM vs 2.5 for neurite elongation) (Figs. 3 and 4). Interestingly, these effects were totally counteracted by the co-administration of BD-1063, confirming that σ_1 receptors are involved in (R,S)-**33** HCl modulation of the NGF effect in PC12 cells and suggesting the σ_1 receptor
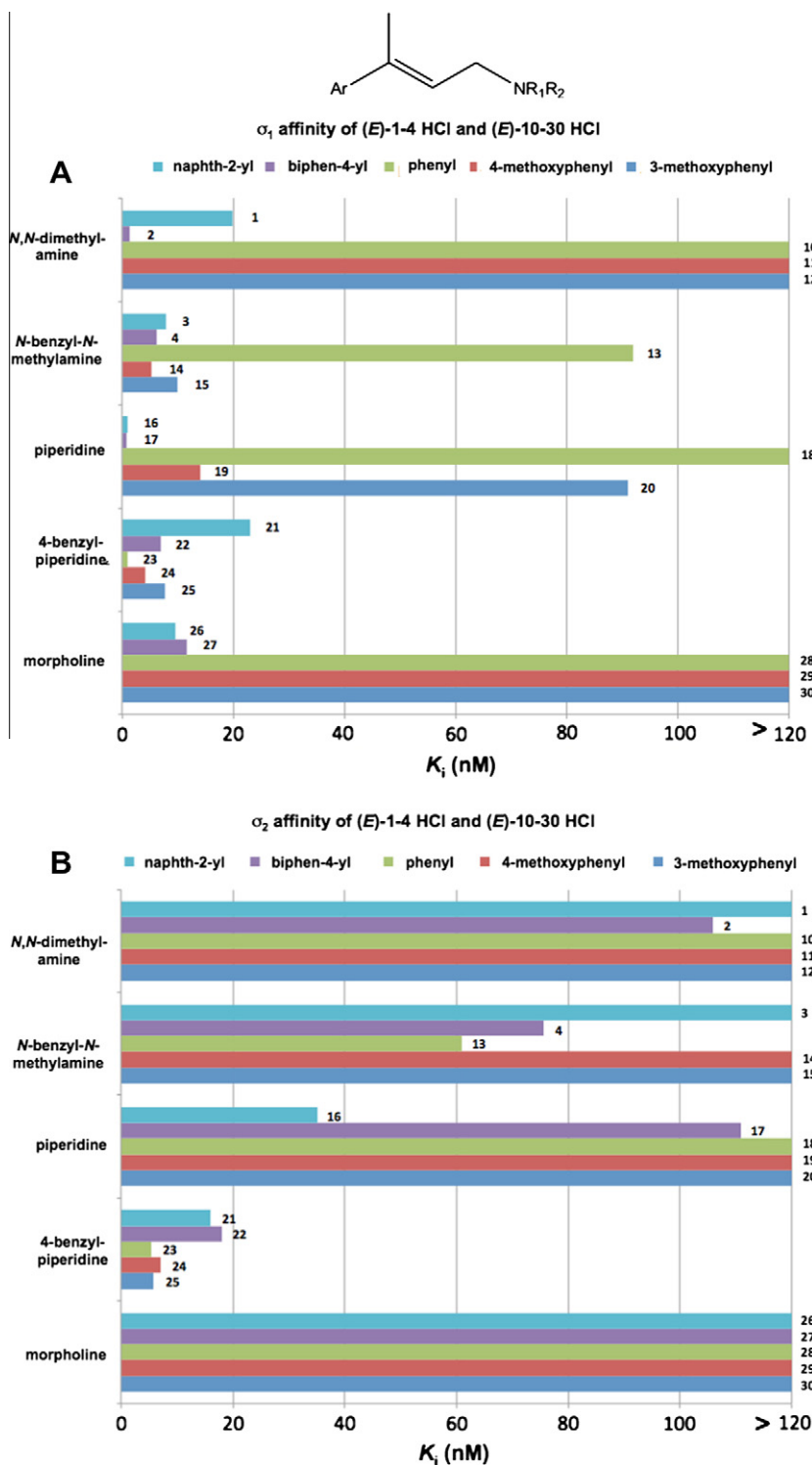
Figure 9. σ_1 (**A**) and σ_2 (**B**) receptor affinity (K_i, nM) of arylalkenylamines (*E*)-**1–4** HCl and (*E*)-**10–30** HCl.

agonist profile. Representative images, in bright field and fluorescence microscopy (cells stained with Alexa Fluor® phalloidin, a marker of F-actin cytoskeleton) are reported in Figure 10. It has to be outlined that, at the concentrations showed to potentiate NGF-induced neurite outgrowth and elongation, (*R,S*)-**33** HCl did not show detrimental effects on PC12 cells. A MTT based citotoxicity assay, performed after treating spontaneously transformed human skin (HaCat) cell line with (*R,S*)-**33** HCl for 48 or 72 h, confirmed these results (see Supplementary data).

As regards to (*E*)-**17** HCl, although it did not significantly enhance NGF-induced neurite outgrowth or elongation, the co-administration of BD-1063 significantly decreased the percentage of cells with neurite outgrowth (Fig. 5). These findings suggest that (*E*)-**17** HCl may be a much weaker agonist than (*R,S*)-**33** HCl on NGF-induced neurite outgrowth and elongation in PC12 cells.

As a part of our work, a threedimensional σ_1 pharmacophore model was finally developed employing GALAHAD methodology. Pharmacophore modeling methods should determine the pattern
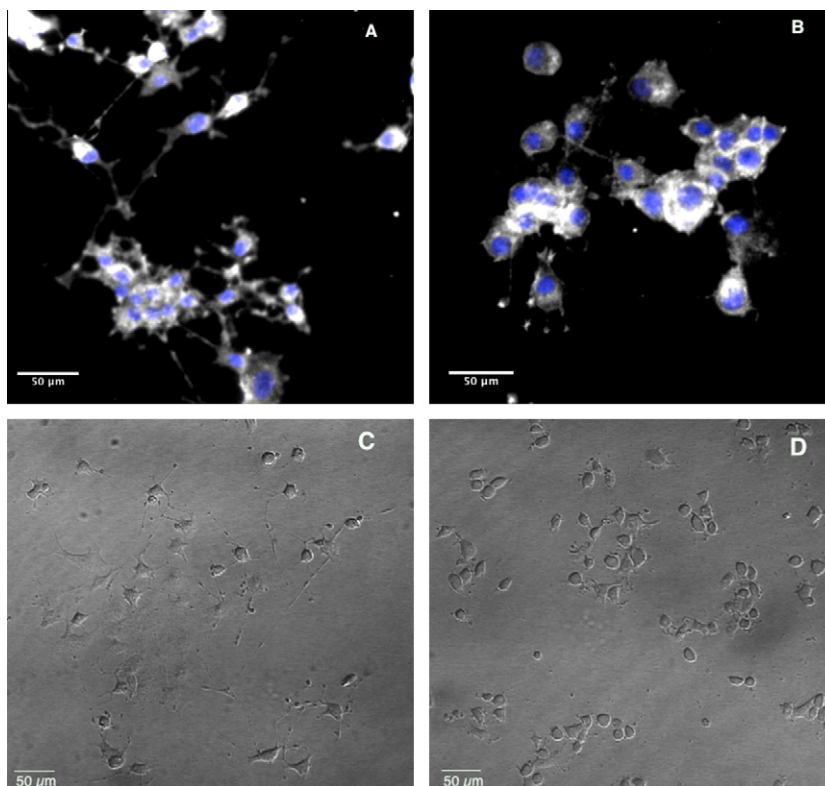
Figure 10. Representative images of F-actin staining with Alexa Fluor® phalloidin in PC12 cells treated with (A) (R,S)-**33** HCl (0.25 μM) or (B) (R,S)-**33** HCl (0.25 μM) and BD-1063 (5 μM). Bright field representative images of PC12 cells treated with (C) (R,S)-**33** HCl (0.25 μM) or (D) (R,S)-**33** HCl (0.25 μM) and BD-1063 (5 μM).

of active compounds and this pattern should exclude the non-active compounds. The quality of a pharmacophore model can be tested by using it to develop predictions of compounds that were not used to build the model. A pharmacophore model is good if: (i) the predictions of the more active compounds that were not used to built the model have a high value; and (ii) the model should be able to identify that the less active compounds are not good ligands of the target.

According to Figure 8 the compounds with experimental $\log(1/K_i)$ above the threshold value −1.4 are the most active compounds. Our model fails in the point (i) for 60% of the tested compounds; this means that our model can lose the detection of active compounds in a virtual screening. On the other hand, the compounds having experimental $\log(1/K_i)$ below −1.4 were defined as the less active compounds. All the compounds with $\log(1/K_i)$ lower than −1.4 were successfully predicted; this means that our model fulfills the point (ii).

In summary, we built a model that identified the less active compounds successfully and identified the 40% of the most active compounds as σ_1 ligands. Accordingly, our model could be successfully employed in a virtual screening study: although some active compounds can be neglected, the model rigorously discards the inactive compounds.

4. Conclusions

In an important extension of previous work, in the present contribution we reported the synthesis, drug-likeness evaluation and in vitro studies of new σ ligands based on the arylalkenylaminic scaffold [compounds (E)-**10–30** HCl]. In this family, molecules generally showed interesting binding properties for σ_1 receptor subtype (K_i values <25 nM) and good σ_1/σ_2 selectivity (>120).

Basing on binding affinity data, a pharmacophore model was developed by using GALAHAD. Interestingly, the developed model was able to discriminate between molecules with and without affinity toward σ_1 receptor subtype and thus to correctly predict σ_1 receptor affinity of new molecules.

Overall biological investigation suggested that the compound to be highlighted is (R,S)-**33** HCl, showing: (i) an excellent σ_1 receptor affinity ($K_i = 0.70 \pm 0.3$ nM); (ii) a high selectivity over σ_2, μ-, and κ-opioid receptors and PCP binding site of the NMDA receptors and (iii) a σ_1 receptor agonist profile. Indeed, in our validated PC12 cell model, it was able to increase both neurite outgrowth and elongation, resulting more effective than the well characterized σ_1 receptor agonist PRE-084. Moreover, (R,S)-**33** HCl is not toxic for PC12 cells and for HaCaT cells at the concentrations shown to potentiate NGF-induced neurite outgrowth and elongation. It has to be outlined that the phospholipase C-γ (PLC-γ), phosphoinositide 3 kinase (PI3K), 38 kDa mitogen activated protein kinase (p38MAPK), c-Jun N-terminal kinase (JNK), and extracellular-signal regulated kinase (ERK) signaling pathways have been recently proved to be involved in the potentiation of NGF-induced neurite outgrowth by σ_1 receptor agonists in PC12 cells;[26] moreover activation of ERK has been found involved in σ_1-agonist mediated neuroprotection in primary neuronal cultures exposed to oxygen-glucose deprivation.[27,28] According to these evidences and based on our biological results, we identified (R,S)-**33** HCl as the optimal candidate for the hit-to-lead process. In particular, our current efforts are directed toward: (i) isolation of **33** pure enantiomers, in order to investigate the role of chirality in both σ receptor binding affinity and efficacy in NGF-induced neurite outgrowth and elongation; (ii) further characterization of the signaling pathways activated by the novel σ_1-agonist (R,S)-**33** HCl and the potential neuroprotective effects of this molecule.

5. Experimental

5.1. Chemistry

5.1.1. General remarks

Unless otherwise specified, commercially available reagents were used as received from the supplier. Solvents were purified according to the guidelines in Purification of Laboratory Chemicals.[29] Pd(0) EnCat™ 30NP (loading = 0.4 mmol/g) and TPPP (loading ~3 mmol/g) were purchased from Sigma–Aldrich. Melting points were measured on SMP3 Stuart Scientific apparatus and are uncorrected Analytical TLC were carried out on silica gel precoated glass-backed plates (Fluka Kieselgel 60 F254, Merck) and visualized by ultra-violet radiation, acidic ammonium molybdate(IV), or potassium permanganate. Flash chromatography was performed with Silica Gel 60 (particle size 230–400 mesh) purchased from NovaChimica. Bond Elute SCX cartridges were purchased from Varian. IR spectra were recorded on a Jasco FT/IR-4100 spectrophotometer; only noteworthy absorptions are given. ^{1}H NMR spectra were measured with an AVANCE 400 spectrometer Bruker, Germany at rt. Chemical shifts (δ) are given in ppm, coupling constants (J) are in Hertz (Hz) and signals are designated as follows: (s) singlet, (br s) broad singlet, (d) doublet, (t) triplet, (q) quartet, and (m) multiplet. TMS was used as internal standard. MS spectra were recorded on a Finnigan LCQ Fleet system (Thermo Finnigan, San Jose, CA, USA), using an ESI source operating in positive ion mode. The purities of target compounds were determined on a Jasco HPLC system equipped with a Jasco autosampler (model AS-2055 plus), a quaternary gradient pump (model PU-2089 plus), and a multiwavelength detector (model MD-2010 plus). The HPLC method used was as follows: column XBridge™ Phenyl, 4.6 mm × 150 mm, 5 μm; column temperature, ambient; flow rate, 1 mL/min; gradient elution, 10% methanol in phosphate buffer (5 mM, pH 7.6) to 90% methanol in phosphate buffer (5 mM, pH 7.6) in 10 min, followed by isocratic elution, 90% methanol in phosphate buffer (5 mM, pH 7.6) for 10 min. All of the final compounds had 95% or greater purity. Elemental analyses (C, H, N) were performed on a Carlo Erba 1106 analyzer and the analysis results were within ±0.4% of the theoretical values.

5.1.2. General procedure for the preparation of compounds 8, 9

A solution of the appropriate amine (8.71 g and 17.5 g for morpholine and 4-benzylpiperidine, respectively; 100 mmol) and but-3-en-2-one (10.5 g, 150 mmol) in PEG 400 (250 g) was stirred at rt for 35 min and then 10% HCl was added until pH 2 was reached. The aqueous phase was washed with dichloromethane (CH_2Cl_2), made alkaline with 1 N NaOH solution (pH 10) and extracted with CH_2Cl_2. The combined organic layers were dried over anhydrous Na_2SO_4 and concentrated in vacuo to give pure 9 (8.65 g, 55% yield) and crude 8, which was further purified by filtration on an alumina pad eluting with ethyl acetate (EtOAc), yielding the desired compound (18.4 g, 75% yield).

5.1.3. 4-(4-Benzylpiperidin-1-yl)butan-2-one (8)

Compound 8 was obtained as a yellow solid: mp 123–124 °C. IR (cm^{-1}): 3077, 3020, 2925–2902, 2795, 1711, 1603, 1490, 1440, 1377, 1357–1245, 1125, 1108–1056, 947, 748, 701. ^{1}H NMR (400 MHz, CDCl$_3$) δ: 1.27 (dd, J = 3.5, 12.0 Hz, 1H), 1.33 (dd, J = 3.5, 12.1 Hz, 1H), 1.53 (ttt, J = 3.3, 7.3, 11.0 Hz, 1H), 1.60–1.69 (m, 2H), 1.92 (dt, J = 2.2, 11.8 Hz, 2H), 2.17 (s, 3H), 2.53 (d, J = 7.1 Hz, 2H), 2.60–2.69 (m, 4H), 2.83–2.91 (m, 2H), 7.11–7.16 (m, 2H), 7.16–7.22 (m, 1H), 7.24–7.31 (m, 2H). MS *m/z* [MH$^+$] 246.04.

5.1.4. 4-Morpholinobutan-2-one (9)

Compound 9 was obtained as a yellow oil. IR (cm^{-1}): 2956–2853, 2807, 1710, 1457–1447, 1358, 1292–1274, 1137, 1115, 1070. ^{1}H NMR (400 MHz, CDCl$_3$) δ: 2.08 (s, 3H), 2.31–2.38 (m, 4H), 2.49–2.59 (m, 4H), 3.56–3.62 (m, 4H). MS *m/z* [MH$^+$] 157.99.

5.1.5. General procedure for the preparation of compounds (*E*)-10–30 hydrochlorides (method I)

t-BuLi (10.1 mL, 17.2 mmol, 1.7 M in pentane) was added dropwise to a solution of the appropriate aromatic precursor (8.58 mmol) in anhydrous diethyl ether (42.9 mL) cooled to −78 °C under nitrogen atmosphere, keeping the temperature for 20 min. The reaction mixture was then slowly allowed to warm to rt. After 1 h stirring, a solution of the appropriate β-aminoketone (6.86 mmol) in dry diethyl ether (10 mL) was added drop-wise at −78 °C. The reaction mixture was slowly allowed to warm to 0 °C and, after 3 h under stirring, quenched with 37% HCl until pH 2 and stirred overnight.

Reaction work-up for compounds **16, 17, 21, 22, 24,** and **27**: the organic phase was separated from the aqueous one containing a white-yellow solid, which was isolated by filtration and dissolved in water. The aqueous solution was then made alkaline with 1 N NaOH (pH 10) and extracted with EtOAc. The combined organic phases were dried over anhydrous Na_2SO_4 and concentrated in vacuo, yielding crude **16, 17, 21, 22, 24,** and **27** as free bases. Compounds **16, 24,** and **27** were then converted into the corresponding hydrochlorides and crystallized from acetone to give pure (*E*)-**16** HCl, (*E*)-**24** HCl, and (*E*)-**27** HCl as white solids. Compounds **17, 21,** and **22** were further purified by crystallization from the appropriate solvent (mixture of methanol/water, 8:2 v/v for compounds **17** and **22**; CH_2Cl_2 for compound **21**) and then converted into the corresponding hydrochloride, which were crystallized from acetone affording pure (*E*)-**17** HCl, (*E*)-**21** HCl, and (*E*)-**22** HCl as white solids.

Reaction work-up for compounds **10–15, 18–20, 23, 25, 26, 28–30**: the organic layer was extracted with 10% HCl and the aqueous phase washed with diethyl ether. The combined acid aqueous phases were then made alkaline with 1 N NaOH (pH 10) and extracted with EtOAc. The organic phases were dried over anhydrous Na_2SO_4, treated with 37% HCl and crystallized from acetone to give the desired pure (*E*) hydrochlorides salts as white solids. For compounds **19** and **29**, a further purification by flash chromatography on silica gel (*n*-hexane/EtOAc/methanol/7 N NH$_3$ in methanol 9:1:0.5:0.1 v/v/v/v and *n*-hexane/EtOAc/diethylamine 5:5:0.1 v/v/v, respectively) was performed prior to salification; crystallization from acetone furnished the expected pure (*E*)-**19** HCl and **29** HCl as white solids.

5.1.6. (*E*)-*N,N*-Dimethyl-3-phenylbut-2-en-1-amine hydrochloride [(*E*)-10 HCl]

White solid (0.57 g, 39% yield), mp 199–200 °C. IR (cm^{-1}): 3113b, 2350, 1548, 1515, 1182, 1020, 950, 870, 757, 691. ^{1}H NMR (400 MHz, CD$_3$OD) δ: 2.22 (d, J = 1.2 Hz, 3H), 2.94 (s, 6H), 4.00 (d, J = 7.8 Hz, 2H), 5.88 (qt, J = 1.2, 7.8 Hz, 1H), 7.31–7.43 (m, 3H), 7.48–7.54 (m, 2H). MS *m/z* [MH$^+$] 176.01. HPLC t_R = 12.06 min, >98.0% pure (λ = 241 nm).

5.1.7. (*E*)-3-(4-Methoxyphenyl)-*N,N*-dimethylbut-2-en-1-amine hydrochloride [(*E*)-11 HCl]

White solid (0.76 g, 46% yield), mp 200–201 °C. IR (cm^{-1}): 3006, 2573, 2362, 2310, 1511, 1250, 1182, 1029, 954, 835. ^{1}H NMR (400 MHz, D$_2$O) δ: 2.02 (d, J = 1.3 Hz, 3H), 2.78 (s, 6H), 3.73 (s, 3H), 3.82 (d, J = 7.8 Hz, 2H), 5.69 (qt, J = 1.3, 7.8 Hz, 1H), 6.87–6.94 (m, 2H), 7.37–7.42 (m, 2H). MS *m/z* [MH$^+$] 206.15. HPLC t_R = 12.06 min, >95.8% pure (λ = 251 nm).

5.1.8. (E)-3-(3-Methoxyphenyl)-N,N-dimethylbut-2-en-1-amine hydrochloride [(E)-12 HCl]

White solid (1.00 g, 60% yield), mp 156–157 °C. IR (cm^{-1}): 3031b, 2364, 1606, 1574, 1424, 1338, 1213, 1051, 950, 869. ^{1}H NMR (400 MHz, D$_2$O) δ: 2.03 (d, J = 1.4 Hz, 3H), 2.79 (s, 6H), 3.73 (s, 3H), 3.84 (d, J = 7.9 Hz, 2H), 5.73 (qt, J = 1.4, 7.8 Hz, 1H), 6.89 (dd, J = 2.3, 8.0 Hz, 1H), 6.95 (t, J = 2.2 Hz, 1H), 7.04 (app. d, J = 7.8 Hz, 1H), 7.27 (t, J = 8.0 Hz, 1H). MS m/z [MH$^+$] 206.01. HPLC t_R = 12.23 min, >98.0% pure (λ = 241 nm).

5.1.9. (E)-N-Benzyl-N-methyl-3-phenylbut-2-en-1-amine hydrochloride [(E)-13 HCl]

White solid (0.83 g, 42% yield), mp 180–181 °C. IR (cm^{-1}): 2884b, 2588, 2503, 2317, 1442, 1338, 1212, 1066, 919, 762. ^{1}H NMR (400 MHz, D$_2$O) δ: 1.94 (s, 3H), 2.71 (s, 3H), 3.84 (br s, 2H), 4.23 (br s, 2H), 5.71 (t, J = 7.8 Hz, 1H), 7.23–7.34 (m, 3H), 7.34–7.43 (m, 7H). MS m/z [MH$^+$] 252.06. HPLC t_R = 13.78 min, >98.0% pure (λ = 241 nm).

5.1.10. (E)-N-Benzyl-3-(4-methoxyphenyl)-N-methylbut-2-en-1-amine hydrochloride [(E)-14 HCl]

White solid (1.18 g, 54% yield), mp 172–173 °C. IR (cm^{-1}): 3031b, 2472, 2363, 2309, 1747, 1604, 1511, 1250, 1025, 830. ^{1}H NMR (400 MHz, D$_2$O) δ: 1.93 (d, J = 1.3 Hz, 3H), 2.71 (s, 3H), 3.72 (s, 3H), 3.83 (br s, 2H), 4.23 (br s, 2H), 5.67 (qt, J = 1.3, 7.8 Hz, 1H), 6.86–6.91 (m, 2H), 7.33–7.45 (m, 7H). MS m/z [MH$^+$] 282.11. HPLC t_R = 13.79 min, >98.0% pure (λ = 251 nm).

5.1.11. (E)-N-Benzyl-3-(3-methoxyphenyl)-N-methylbut-2-en-1-amine hydrochloride [(E)-15 HCl]

White solid (0.96 g, 44% yield), mp 149–150 °C. IR (cm^{-1}): 2949b, 2514, 2363, 2310, 1598, 1425, 1294, 1038, 912, 862. ^{1}H NMR (400 MHz, D$_2$O) δ: 1.93 (d, J = 1.3 Hz, 3H), 2.72 (s, 3H), 3.72 (s, 3H), 3.84 (br d, J = 7.5 Hz, 2H), 4.24 (br s, 2H), 5.71 (qt, J = 1.3, 7.7 Hz, 1H), 6.87 (dd, J = 2.6, 8.2 Hz, 1H), 6.91 (t, J = 2.3 Hz, 1H), 7.00 (app d, J = 8.3 Hz, 1H), 7.25 (t, J = 8.0 Hz, 1H), 7.34–7.45 (m, 5H). MS m/z [MH$^+$] 282.04. HPLC t_R = 13.89 min, >98.0% pure (λ = 241 nm).

5.1.12. (E)-1-(3-(Naphthalen-2-yl)but-2-en-1-yl)piperidine hydrochloride [(E)-16 HCl]

White solid (1.59 g, 77% yield), mp 209–210 °C. IR (cm^{-1}): 3058, 2931, 2859, 2607, 2484, 2413–2395, 1646–1595, 1439, 1399–1280, 1160–1078, 1038, 957–944, 896, 850, 818, 741 ^{1}H NMR (400 MHz, D$_2$O) δ 1.22–1.40 (m, 1H), 1.46–1.64 (m, 2H), 1.64–1.74 (m, 1H), 1.74–1.86 (m, 2H), 2.05 (s, 3H), 2.78 (app. t, J = 12.1 Hz, 2H), 3.38 (app. d, J = 11.5 Hz, 2H), 3.72 (d, J = 7.8 Hz, 2H), 5.76 (t, J = 7.8 Hz, 1H), 7.39–7.47 (m, 2H), 7.50 (dd, J = 1.8, 7.7 Hz, 1H), 7.73–7.86 (m, 4H). MS m/z [MH$^+$] 266.13. HPLC t_R = 14.14 min, >98.0% pure (λ = 241 nm).

5.1.13. (E)-1-(3-([1,1'-Biphenyl]-4-yl)but-2-en-1-yl)piperidine hydrochloride [(E)-17 HCl]

White solid (1.24 g, 55% yield), mp 235–236 °C. IR (cm^{-1}): 3038–2974, 2943, 2612, 2505, 2413, 1651–1514, 1485, 1438, 1400, 1282, 950, 832, 763, 695. ^{1}H NMR (400 MHz, D$_2$O) δ: 1.26–1.44 (m, 1H), 1.47–1.67 (m, 2H), 1.67–1.78 (m, 1H), 1.79–1.90 (m, 2H), 2.07 (s, 3H), 2.87 (app. t, J = 12.5 Hz, 2H), 3.45 (app. d, J = 12.0 Hz, 2H), 3.81 (d, J = 7.8 Hz, 2H), 5.79 (t, J = 7.7 Hz, 1H), 7.31–7.38 (m, 1H), 7.39–7.47 (m, 2H), 7.49–7.55 (m, 2H), 7.58–7.66 (m, 4H). MS m/z [MH$^+$] 292.12. HPLC t_R = 14.73 min, >98.0% pure (λ = 271 nm).

5.1.14. (E)-1-(3-Phenylbut-2-en-1-yl)piperidine hydrochloride [(E)-18 HCl]

White solid (0.52 g, 30% yield), mp 235–236 °C. IR (cm^{-1}): 2943, 2609, 2489, 1649, 1434–1454, 947, 846, 758, 691. ^{1}H NMR

(400 MHz, D$_2$O) δ: 1.24–1.39 (m, 1H), 1.47–1.62 (m, 2H), 1.63–1.72 (m, 1H), 1.73–1.86 (m, 2H), 2.00 (s, 3H), 2.82 (app. t, J = 12.0 Hz, 2H), 3.40 (app. d, J = 12.1 Hz, 2H), 3.75 (d, J = 7.8 Hz, 2H), 5.67 (t, J = 7.7 Hz, 1H), 7.21–7.34 (m, 3H), 7.34–7.42 (m, 2H). MS m/z [MH$^+$] 216.04 HPLC t_R = 13.25 min, >98.0% pure (λ = 241 nm).

5.1.15. (E)-1-(3-(3-Methoxyphenyl)but-2-en-1-yl)piperidine hydrochloride [(E)-20 HCl]

White solid (1.16 g, 60% yield), mp 163–165 °C. IR (cm^{-1}): 2998–3068, 2944, 2834–2856, 2611, 2507, 1600, 1572, 1486, 1427, 1291, 1211, 1158, 1047, 941–958, 878, 827, 780, 697. ^{1}H NMR (400 MHz, D$_2$O) δ: 1.32–1.46 (m, 1H), 1.55–1.70 (m, 2H), 1.70–1.79 (m, 1H), 1.82–1.92 (m, 2H), 2.06 (d, J = 1.3 Hz, 3H), 2.80 (dt, J = 2.7, 12.7 Hz, 2H), 3.48 (app. d, J = 12.1 Hz, 2H), 3.77 (s, 3H), 3.82 (d, J = 7.9 Hz, 2H), 5.75 (qt, J = 1.3, 7.9 Hz, 1H), 6.93 (dd, J = 2.5, 8.1 Hz, 1H), 6.99 (t, J = 2.3 Hz, 1H), 7.10 (d, J = 8.0 Hz, 1H), 7.31 (t, J = 8.0 Hz, 1H). MS m/z [MH$^+$] 246.09. HPLC t_R = 13.39 min, >98.0% pure (λ = 241 nm).

5.1.16. (E)-4-Benzyl-1-(3-(naphthalen-2-yl)but-2-en-1-yl)piperidine hydrochloride [(E)-21 HCl]

White solid (0.81 g, 30% yield), mp 221–222 °C. IR (cm^{-1}) 2977–3049, 2926, 2848, 2514, 1597, 1482, 1434–1453, 1157–1287, 1039, 940, 895, 855, 819, 744, 698. ^{1}H NMR (400 MHz, CD$_3$OD) δ: 1.41–1.59 (m, 2H), 1.84–1.99 (m, 3H), 2.28 (d, J = 1.2 Hz, 3H), 2.62 (d, J = 6.5 Hz, 2H), 3.00 (app. t, J = 12.8 Hz, 2H), 3.61 (app. d, J = 12.8 Hz, 2H), 3.98 (d, J = 7.7 Hz, 2H), 6.00 (qt, J = 1.2, 7.7 Hz, 1H), 7.14–7.22 (m, 3H), 7.23–7.32 (m, 2H), 7.43–7.52 (m, 2H), 7.63 (dd, J = 1.8, 8.6 Hz, 1H), 7.79–7.90 (m, 3H), 7.93 (s, 1H). MS m/z [MH$^+$] 356.21. HPLC t_R = 16.21 min, >98.0% pure (λ = 241 nm).

5.1.17. (E)-4-Benzyl-1-(3-([1,1'-biphen]-4-yl)but-2-en-1-yl)piperidine hydrochloride [(E)-22 HCl]

White solid (1.38 g, 48% yield), mp 237–240 °C. IR (cm^{-1}): 3085–2979, 2926, 2488, 1641–1580, 1484–1401, 1273–1160, 1038, 943, 835, 765–748, 698. ^{1}H NMR (400 MHz, CD$_3$OD) δ: 1.47–1.62 (m, 2H), 1.88–2.02 (m, 3H), 2.23 (d, J = 1.3 Hz, 3H), 2.67 (d, J = 6.7 Hz, 2H), 3.03 (app. t, J = 12.0 Hz, 2H), 3.59 (app. d, J = 12.0 Hz, 2H), 3.97 (d, J = 7.7 Hz, 2H), 5.94 (qt, J = 1.3, 7.7 Hz, 1H), 7.19–7.24 (m, 3H), 7.27–7.39 (m, 3H), 7.42–7.49 (m, 2H), 7.56–7.61 (m, 2H), 7.62–7.68 (m, 4H). MS m/z [MH$^+$] 382.19. HPLC t_R = 17.17 min, >98.0% pure (λ = 271 nm).

5.1.18. (E)-4-Benzyl-1-(3-phenylbut-2-en-1-yl)piperidine hydrochloride [(E)-23 HCl]

White solid (1.06 g, 45% yield), mp 220–222 °C. IR (cm^{-1}): 3055–3025, 2922, 2493, 1650–1598, 1442–1455, 758, 744, 693. ^{1}H NMR (400 MHz, D$_2$O) δ: 1.32–1.47 (m, 2H), 1.77–1.89 (m, 3H), 2.06 (d, J = 1.3 Hz, 3H), 2.55 (d, J = 6.7 Hz, 2H), 2.88 (app. t, J = 12.7 Hz, 2H), 3.51 (app. d, J = 12.8 Hz, 2H), 3.83 (d, J = 7.9 Hz, 2H), 5.75 (qt, J = 1.3, 7.9 Hz, 1H), 7.17–7.25 (m, 3H), 7.27–7.40 (m, 5H), 7.42–7.48 (m, 2H). MS m/z [MH$^+$] 306.17. HPLC t_R = 15.05 min, >95.8% pure (λ = 241 nm).

5.1.19. (E)-4-Benzyl-1-(3-(4-methoxyphenyl)but-2-en-1-yl)piperidine hydrochloride [(E)-24 HCl]

White solid (1.28 g, 50% yield), mp 190–193 °C. IR (cm^{-1}): 3030–3061, 2837–2973, 2506, 1605, 1511, 1449, 1242, 1027, 821, 751, 702. ^{1}H NMR (400 MHz, D$_2$O) δ: 1.30–1.47 (m, 2H), 1.74–1.89 (m, 3H), 2.03 (s, 3H), 2.55 (d, J = 6.4 Hz, 2H), 2.86 (app. t, J = 12.4 Hz, 2H), 3.49 (app. d, J = 12.6 Hz, 2H), 3.77 (s, 3H), 3.81 (d, J = 7.7 Hz, 2H), 5.70 (t, J = 7.6 Hz, 1H), 6.91–7.00 (m, 2H), 7.16–7.25 (m, 3H), 7.26–7.35 (m, 2H), 7.38–7.46 (m, 2H). MS m/z [MH$^+$] 336.25. HPLC t_R = 15.10 min, >98.0% pure (λ = 251 nm).

5.1.20. (*E*)-4-Benzyl-1-(3-(3-methoxyphenyl)but-2-en-1-yl)piperidine hydrochloride [(*E*)-25 HCl]

White solid (1.15 g, 45% yield), mp 169–173 °C. IR (cm⁻¹): 3079–3024, 2998–2919, 2490, 1576, 1454–1432, 1287, 1210, 1046, 776, 743, 698, 692. ¹H NMR (400 MHz, D₂O) δ: 1.32–1.47 (m, 2H), 1.74–1.90 (m, 3H), 2.05 (s, 3H), 2.55 (d, *J* = 6.7 Hz, 2H), 2.87 (app. t, *J* = 12.6 Hz, 2H), 3.50 (app. d, *J* = 11.8 Hz, 2H), 3.78 (s, 3H), 3.82 (d, *J* = 7.9 Hz, 2H), 6.75 (t, *J* = 7.8 Hz, 1H), 6.93 (dd, *J* = 2.5, 8.2 Hz, 1H), 6.97–7.01 (m, 1H), 7.03–7.09 (m, 1H), 7.16–7.24 (m, 3H), 7.26–7.35 (m, 3H). MS *m/z* [MH⁺] 336.15. HPLC *t*_R = 15.23 min, >98.0% pure (λ = 241 nm).

5.1.21. (*E*)-4-(3-(Naphthalen-2-yl)but-2-en-1-yl)morpholine hydrochloride [(*E*)-26 HCl]

White solid (1.19 g, 57% yield), mp 221–222 °C. IR (cm⁻¹): 3056, 2939–2976, 2453–2526, 1639, 1399–1440, 1123, 1081, 961, 812, 740. ¹H NMR (400 MHz, D₂O) δ: 2.13 (d, *J* = 1.2 Hz, 3H), 2.99–3.57 (br, 4H), 3.60–4.19 (br, 4H), 3.88 (d, *J* = 7.9 Hz, 2H), 5.83 (qt, *J* = 1.2, 8.0 Hz, 1H), 7.46–7.51 (m, 2H), 7.56 (dd, *J* = 1.8, 8.7 Hz, 1H), 7.80–7.87 (m, 3H), 7.88 (d, *J* = 1.2 Hz, 1H). MS *m/z* [MH⁺] 268.01. HPLC *t*_R = 13.16 min, >98.0% pure (λ = 241 nm).

5.1.22. (*E*)-4-(3-([1,1′-Biphen]-4-yl)but-2-en-1-yl)morpholine hydrochloride [(*E*)-27 HCl]

White solid (0.95 g, 42% yield), mp 244–252 °C. IR (cm⁻¹): 2975–3075, 2865, 2519, 2401–2445, 1516–1644, 1485, 1443, 1402, 1260, 1121, 1079, 959, 827, 762, 693. ¹H NMR (400 MHz, D₂O) δ: 2.06 (s, 3H), 3.05–3.19 (m, 2H), 3.36–3.50 (m, 2H), 3.60–3.76 (m, 2H), 3.89 (d, *J* = 8.0 Hz, 2H), 3.95–4.06 (m, 2H), 5.77 (t, *J* = 7.9 Hz, 1H), 7.28–7.35 (m, 1H), 7.37–7.44 (m, 2H), 7.47–7.53 (m, 2H), 7.56–7.64 (m, 4H). MS *m/z* [MH⁺] 294.12. HPLC *t*_R = 13.64 min, >98.0% pure (λ = 271 nm).

5.1.23. (*E*)-4-(3-Phenylbut-2-en-1-yl)morpholine hydrochloride [(*E*)-28 HCl]

White solid (0.84 g, 48% yield), mp 203–212 °C. IR (cm⁻¹): 3050, 2871–2983, 2476–2538, 1437, 1258, 1125, 1082, 959, 763. ¹H NMR (400 MHz, D₂O) δ: 2.04 (s, 3H), 3.02–3.44 (br, 4H), 3.63–4.01 (br, 4H), 3.86 (d, *J* = 7.9 Hz, 2H), 5.71 (t, *J* = 7.8 Hz, 1H), 7.23–7.36 (m, 3H), 7.37–7.46 (m, 2H). MS *m/z* [MH⁺] 218.05. HPLC *t*_R = 12.25 min, >98.0% pure (λ = 241 nm).

5.1.24. (*E*)-4-(3-(3-Methoxyphenyl)but-2-en-1-yl)morpholine hydrochloride [(*E*)-30 HCl]

White solid (0.76 g, 39% yield), mp 158–163 °C. IR (cm⁻¹): 3021, 2834–2999, 2454–2469, 1580, 1444–1464, 1213, 1125, 1080, 1032, 962, 865, 840, 783, 709, 689. ¹H NMR (400 MHz, D₂O) δ: 2.01 (d, *J* = 1.1 Hz, 3H), 2.99–3.45 (br, 4H), 3.56–3.95 (br, 4H), 3.71 (s, 3H), 3.85 (d, *J* = 7.9 Hz, 2H), 5.69 (qt, *J* = 1.2, 7.9 Hz, 1H), 6.87 (dd, *J* = 2.2, 8.2 Hz, 1H), 6.93 (t, *J* = 2.1 Hz, 1H), 7.00 (d, *J* = 7.9 Hz, 1H), 7.24 (t, *J* = 8.0 Hz, 1H). MS *m/z* [MH⁺] 248.02. HPLC *t*_R = 12.29 min, >98.0% pure (λ = 241 nm).

5.1.25. Preparation of compounds (*E*)-19, 29 hydrochlorides (method II)

t-BuLi (10.1 mL, 17.2 mmol, 1.7 M in pentane) was added dropwise to a solution of the 1-bromo-4-methoxy-benzene (1.60 g, 8.58 mmol) in anhydrous diethyl ether (42.9 mL) cooled to −78 °C under nitrogen atmosphere, keeping the temperature for 20 min. The reaction mixture was then slowly allowed to warm to rt. After 1 h under stirring a solution of the appropriate β-aminoketone (1.06 g and 1.08 g for compounds **7** and **9**, respectively; 6.86 mmol) in dry diethyl ether (10 mL) was then added drop-wise at −78 °C. The reaction mixture was slowly allowed to warm to 0 °C, stirred for 3 h and then quenched with water (15 mL). The mixture was added with 5% ᴅʟ-tartaric acid until pH 4 and washed

with diethyl ether; the aqueous phase was then made alkaline with 1 N NaOH (pH 10) and extracted with EtOAc. The combined organic phases were dried over anhydrous Na₂SO₄ and evaporated under reduced pressure affording pure (*R,S*)-31 and crude (*R,S*)-32, which was further purified by flash column chromatography on silica gel (*n*-hexane/EtOAc/diethylamine 5:5:0.1 v/v/v).

The alcohols (*R,S*)-31 or (*R,S*)-32 (0.53 g, 2.0 mmol) dissolved in CH₂Cl₂ (10 mL) were then added to a freshly prepared solution of TPPP (1.00 g, 3.0 mmol) and iodine (0.76 g, 3.0 mmol) in CH₂Cl₂ (24 mL). The mixture was further stirred at rt for 48 h. Aqueous 5% NaHSO₃ was added and after 10 min under stirring the mixture was filtered through a pad of Celite®. The organic phase was washed with 1 N NaOH, dried over anhydrous Na₂SO₄ and concentrated under reduced pressure yielding crude **19** and **29**, which were converted into the corresponding hydrochlorides and crystallized from acetone, providing pure (*E*)-**19** HCl and (*E*)-**29** HCl.

5.1.26. (*R,S*)-2-(4-Methoxyphenyl)-4-(piperidin-1-yl)butan-2-ol [(*R,S*)-31]

Yellow oil (1.17 g, 65% yield). IR (cm⁻¹): 3187, 2930, 2805–2850, 1609, 1508, 1244, 1035, 829. ¹H NMR (400 MHz, DMSO) δ: 1.26–1.37 (m, 2H), 1.32 (s, 3H), 1.38–1.50 (m, 4H), 1.71–1.89 (m, 2H), 2.05–2.17 (m, 4H), 2.20–2.38 (br, 2H), 3.69 (s, 3H), 5.92–6.20 (br s, 1H, exchanges with D₂O), 6.82 (d, *J* = 8.7 Hz, 2H), 7.29 (d, *J* = 8.7 Hz, 2H). MS *m/z* [MH⁺] 264.08.

5.1.27. (*R,S*)-2-(4-Methoxyphenyl)-4-morpholinobutan-2-ol [(*R,S*)-32]

Yellow oil (1.00 g, 55% yield). IR (cm⁻¹): 3154b, 2955, 2817, 1609, 1508, 1243, 1115, 1031, 830. ¹H NMR (400 MHz, DMSO) δ: 1.40 (s, 3H), 1.73–1.81 (m, 2H), 2.14–2.26 (m, 2H), 2.28–2.37 (m, 4H), 3.51–3.63 (m, 4H), 3.77 (s, 3H), 5.74–5.88 (br s, 1H, exchanges with D₂O), 6.82 (d, *J* = 7.3 Hz, 2H), 7.35 (d, *J* = 7.3 Hz, 2H). MS *m/z* [MH⁺] 266.04.

5.1.28. (*E*)-1-(3-(4-Methoxyphenyl)but-2-en-1-yl)piperidine hydrochloride [(*E*)-19 HCl]

White solid (0.27 g, 48% yield, method II), mp 210–212 °C. IR (cm⁻¹): 2934, 2614, 2520, 1607, 1509, 1464, 1454, 1287, 1244, 1173, 1033, 958, 830, 817. ¹H NMR (400 MHz, D₂O) δ: 1.31–1.44 (m, 1H), 1.53–1.68 (m, 2H), 1.69–1.78 (m, 1H), 1.80–1.91 (m, 2H), 2.04 (s, 3H), 2.88 (dt, *J* = 2.5, 12.6 Hz, 2H), 3.46 (app. d, 2H), 3.76 (s, 3H), 3.80 (d, *J* = 8.0 Hz, 2H), 5.71 (t, *J* = 7.9 Hz, 1H), 6.94 (d, *J* = 8.8 Hz, 2H), 7.42 (d, *J* = 8.8 Hz, 2H). MS *m/z* [MH⁺] 246.01. HPLC *t*_R = 13.27 min, >98.0% pure (λ = 251 nm).

5.1.29. (*E*)-4-(3-(4-Methoxyphenyl)but-2-en-1-yl)morpholine hydrochloride [(*E*)-29 HCl]

White solid (0.30 g, 53% yield, method II), mp 209–210 °C. IR (cm⁻¹): 3000–3032, 2934, 2866, 2433, 1512, 1244, 1128, 1026, 970, 827. ¹H NMR (400 MHz, D₂O) δ: 2.00 (d, *J* = 1.2 Hz, 3H), 3.09–3.33 (br, 4H), 3.71 (s, 3H), 3.73–3.94 (br, 4H), 3.82 (d, *J* = 8.0 Hz, 2H), 5.66 (qt, *J* = 1.4, 8.0 Hz, 1H), 6.88 (d, *J* = 8.8 Hz, 2H), 7.37 (d, *J* = 8.8 Hz, 2H). MS *m/z* [MH⁺] 248.02. HPLC *t*_R = 12.25 min, >98.0% pure (λ = 251 nm).

5.1.30. Preparation of (*R,S*)-1-(3-([1,1′-biphen]-4-yl)butyl)piperidine [(*R,S*)-33]

Prior to use, Pd(0) EnCat™ 30NP (supplied as a water wet solid with water content 45% w/w) was washed thoroughly with absolute ethanol to remove water. Pre-washed Pd(0) EnCat™ 30NP (0.21 g, 0.2 equiv) was added to a stirred solution of (*E*)-**17** as free base (0.12 g, 0.41 mmol) in absolute ethanol (21 mL) and the reaction mixture was left at rt in hydrogen atmosphere (balloon) for 22 h. The catalyst was then filtered off and washed with absolute ethanol; the filtrate was loaded on SCX cartridge and eluted with

1 N NH$_3$ in methanol; the organic phase was finally evaporated in vacuo to give pure (R,S)-**33** as free base (yellow oil, 0.072 g, 60% yield). IR (cm^{-1}): 3055, 3027, 2929, 2851, 2799, 2762, 1600, 1486, 1450, 1154, 1119.835, 764. ^{1}H NMR (CDCl$_3$) δ 1.31 (d, J = 7.0 Hz, 3H), 1.39–1.49 (m, 2H), 1.55–1.64 (m, 4H), 1.79–1.92 (m, 2H), 2.21 (ddd, J = 5.8, 9.9, 12.1 Hz, 1H), 2.29–2.46 (br, 4H), 2.31 (ddd, J = 6.2, 9.8, 12.1 Hz, 1H), 2.78 (sextet, J = 7.2 Hz, 1H), 7.28 (d, J = 8.1 Hz, 2H), 7.32–7.38 (m, 1H), 7.42–7.48 (m, 2H), 7.54 (d, J = 8.2 Hz, 2H), 7.59–7.64 (m, 2H). MS m/z [MH$^+$] 294.26. HPLC t_R = 14.82 min, >95.7% pure (λ = 241 nm).

5.2. Biology

5.2.1. Sigma receptor binding assays

Crude membranes were prepared as previously described.[30,31] The protein concentration of the membrane preparations was determined by the Lowry method and the membranes were stored at −80 °C until use. σ_1 Binding affinity was determined incubating membrane aliquots (400 μL, 500 μg protein) at 37 °C for 150 min, with 3 nM [^{3}H]-(+)-pentazocine (45 Ci/mmol) and nine different concentrations of test ligand in assay buffer (50 mM Tris–HCl, pH 7.4) to a final volume of 1 mL. Haloperidol at 10 μM was used to measure the nonspecific binding. For the σ_2 binding assays the membranes (300 μL, 360 μg protein) were incubated at rt for 120 min with 3 nM [^{3}H]DTG (31 Ci/mM) in the presence of (+)-SKF10,047 (0.4 μM) and nine different concentrations of test compound. Incubation was carried out in 50 mM Tris–HCl (pH 8.0) to a final volume of 0.5 mL. Nonspecific binding was evaluated in the presence of 5 μM DTG. After incubation the samples were filtered through Whatman GF/B glass fiber filters, presoaked in a 0.5% polyethyleneimine solution. The filters were washed two times each, with 4 mL of suitable ice-cold buffer and the radioactivity was counted in 4 mL of 'Ultima Gold MV' in a 1414 Winspectral Perkin-Elmer Wallac liquid scintillation counter. K_i values for the tested compounds were calculated using the EBDALIGAND program 34 purchased from Elsevier/Biosoft.

5.2.2. Opioid receptor binding assays

5.2.2.1. Materials and general procedures.
The guinea pig brains were commercially available (Harlan-Winkelmann, Borchen, Germany). Homogenizer: Elvehjem Potter (B. Braun Biotech International, Melsungen, Germany). Centrifuge: High-speed cooling centrifuge model Sorvall RC-5C plus (Thermo Fisher Scientific, Langenselbold, Germany). Filter: Printed Filtermat Typ A and B (Perkin Elmer LAS, Rodgau-Jügesheim, Germany), presoaked in 0.5% aqueous polyethylenimine for 2 h at room temperature before use. The filtration was carried out with a MicroBeta FilterMate-96 Harvester (Perkin Elmer). The scintillation analysis was performed using Meltilex (Typ A or B) solid scintillator (Perkin Elmer). The solid scintillator was melted on the filtermat at a temperature of 95 °C for 5 min. After solidifying of the scintillator at rt, the scintillation was measured using a MicroBeta Trilux scintillation analyzer (Perkin Elmer). The overall counting efficiency was 20%. All experiments were carried out in triplicates using standard 96-well-multiplates (Diagonal, Muenster, Germany). The IC$_{50}$ values were determined in competition experiments with at least six concentrations of the test compounds and were calculated with the program GraphPad Prism® 3.0 (GraphPad Software, San Diego, CA, USA) by non-linear regression analysis. The K_i values were calculated according to the formula of Cheng and Prusoff.

5.2.2.2. Preparation of the tissue.
5 guinea pig brains (μ- and κ-opioid receptor assay) were homogenized with the potter (500–800 rpm, 10 up-and-down strokes) in 6 volumes of cold 0.32 M sucrose. The suspension was centrifuged at 1200×g for 10 min at 4 °C. The supernatant was separated and centrifuged at 23.500×g

for 20 min at 4 °C. The pellet was resuspended in 5-6 volumes of buffer (50 mM TRIS, pH 7.4) and centrifuged again at 23.500×g (20 min, 4 °C). This procedure was repeated twice. The final pellet was resuspended in 5-6 volumes of buffer, the protein concentration was determined according to the method of Bradford using bovine serum albumin as standard and subsequently the preparation was frozen (−80 °C) in 1.5 mL portions containing about 1.5 mg protein/mL.

5.2.2.3. μ-Opioid receptor binding assay.
The test was performed with the radioligand [^{3}H]-DAMGO (51 Ci/mmol, Perkin Elmer LAS). The thawed membrane preparation (about 75 μg of the protein) was incubated with various concentrations of test compounds, 1 nM [^{3}H]-DAMGO and TRIS-MgCl$_2$-PMSF-buffer (50 mM, 8 mM MgCl$_2$, 400 μM PMSF, pH 7.4) in a total volume of 200 μL for 150 min at 37 °C. The incubation was terminated by rapid filtration through the presoaked filtermats using a cell harvester. After washing each well five times with 300 μL of water, the filtermats were dried at 95 °C. The bound radioactivity trapped on the filters was counted as described above. The non-specific binding was determined with 10 μM unlabeled naloxone. The K_d-value of DAMGO is 0.57 nM.

5.2.2.4. κ-Opioid receptor binding assay.
The test was performed with the radioligand [^{3}H]-U 69,593 (55 Ci/mmol, Amersham, Little Chalfont, UK). The thawed membrane preparation (about 75 μg of the protein) was incubated with various concentrations of test compounds, 1 nM [^{3}H]-U 69,593, and TRIS–MgCl$_2$-buffer (50 mM, 8 mM MgCl$_2$, pH 7.4) in a total volume of 200 μL for 150 min at 37 °C. The incubation was terminated by rapid filtration through the presoaked filtermats using a cell harvester. After washing each well five times with 300 μL of water, the filtermats were dried at 95 °C. The bound radioactivity trapped on the filters was counted as described above. The non-specific binding was determined with 10 μM unlabeled U 69,593. The K_d-value of U 69,593 is 0.69 nM.

5.2.3. Binding studies at the PCP binding site of the NMDA receptor

5.2.3.1. Preparation of the receptor material.
Fresh pig brain cortex was homogenized with the potter (500–800 rpm, 10 up-and-down strokes) in 6 volumes of cold 0.32 M sucrose. The suspension was centrifuged at 1200g for 10 min at 4 °C. The supernatant was separated and centrifuged at 23,500g for 20 min at 4 °C. The pellet was resuspended in buffer [5 mM Tris–acetate with 1 mM ethylenediaminetetraacetic acid (EDTA), pH 7.5] and centrifuged again at 31,000g (20 min, 4 °C). This procedure was repeated twice. The final pellet was resuspended in buffer, the protein concentration was determined according to the method of Bradford[32] using bovine serum albumin as standard, and subsequently the preparation was frozen (−83 °C) in 1.5 mL portions containing about 0.8 mg protein/mL.

5.2.3.2. Performance of the assay.
The test was performed with the radioligand [^{3}H]-(+)-MK-801 (22.0 Ci/mmol; Perkin–Elmer). The thawed membrane preparation (about 100 μg of the protein) was incubated with various concentrations of test compounds, 2 nM [^{3}H]-(+)-MK-801, and TRIS/EDTA-buffer (5 mM/1 mM pH 7.5) in a total volume of 200 μL for 150 min at rt. The incubation was terminated by rapid filtration through the presoaked filtermats using the cell harvester. After washing each well five times with 300 μL of water, the filtermats were dried at 95 °C. Subsequently, the solid scintillator was placed on the filtermat and melted at 95 °C. After 5 min, the solid scintillator was allowed to solidify at rt. The bound radioactivity trapped on the filters was counted in the scintillation analyzer. The non-specific binding

was determined with 10 μM (+)-MK-801. The K_d value of the radi-oligand [^{3}H]-(+)-MK-801 is 2.26 nM.

5.2.4. NGF neurite outgrowth in PC12 cells

5.2.4.1. Cell culture. PC12 cells were cultured at 37 °C, 5% CO_2 with RPMI medium supplemented with 5% heat-inactivated fetal bovine serum (FBS), 10% heat-inactivated horse serum (HS), 200 mM glutamine, and 1% penicillin/streptomycin. The medium was changed two or three times a week. When NGF with or without the compounds to be tested, had to be added, cells were detached from the culture dishes, centrifuged at 150g for 5 min, and plated at 0.25×10^4 cells/cm^2 onto 19 mm-wide glass cover-slips coated with poly-D-lysine in 12-well tissue culture plates. Twenty-four hours after plating, the medium was replaced with RPMI medium containing 0.5% HS, 200 mM glutamine, 1% penicil-lin/streptomycin and with NGF (2.5 ng/mL) with or without drugs. Compounds (R,S)-**33** HCl and (E)-**17** HCl were dissolved in DMSO (1 mg/100 μL and 1 mg/180 μL, respectively), diluted with apyro-genic H_2O to 1 mM solution and added to the cell medium to reach the selected final concentrations. The well characterized σ_1 recep-tor agonist PRE-084 and antagonist BD-1063 at 10 mM stock solu-tions were diluted in apyrogenic H_2O to 1 mM solutions and then added to the cell medium. In some experiments, BD-1063 was co-administered with (R,S)-**33** HCl, (E)-**17** HCl or PRE-084 at a final concentration of 5 μM.

5.2.4.2. Quantification of neurite outgrowth and length. Five days after incubation with NGF (2.5 ng/mL) with or without (R,S)-**33** HCl and (E)-**17** HCl, PC12 cells, grown on glass coverslips were fixed at rt for 15 min in phosphate-buffered saline (PBS) con-taining 4% (wt/vol) paraformaldehyde. Morphometric analysis was performed on digitized images of fixed cells taken under phase-contrast illumination with an inverted microscope (Optika) linked to a digital camera or with a laser scanning confocal system (TCP-SP2, Leica). Images of six fields per coverslip were taken at 10× or 40× magnification, with an average of 200–20 cells per field. At least three independent experiments were performed for each con-dition. Neurite outgrowth and elongation was scored by measuring the percentage of differentiated cells bearing at least one neurite with a length equal to the cell body diameter and following the length of the neurite from the cell body to the tip. The cell counting and neurite length measurements were performed in a blinded manner by two independent examiners using Image Tool software.

5.2.4.3. Immunocytochemistry. PC12 cells were fixed with 4% paraformaldehyde, washed three times with PBS and then perme-abilized for 5 min with PBS containing 0.2% (wt/vol) Triton X-100. The cells were washed with PBS and blocked with 1.5% bovine ser-um albumin (BSA) in PBS for 1 h. For F-actin visualization, the cells were incubated for 30 min with Alexa Fluor® 633 phalloidin, a high-affinity F-actin probe (Molecular Probes, Invitrogen), diluted in 1% BSA in PBS (1 U/200 μl). At the end of the incubation, cells were counterstained with Hoechst 33342 (1 μM) and washed once in distilled water. The coverslips were mounted with Mowiol/Dab-co on glass slides. All procedures were performed at rt. Alexa Fluor® 633 phalloidin staining was viewed with an Olympus CX31 microscopy equipped with FRAEN AFTER fluorescence UV and RED cassettes and with a Scion CFW-1312M digital camera. Image J software was utilized for image acquisition.

5.2.4.4. Citotoxicity test. In vitro spontaneously transformed keratinocytes from histologically normal human skin (HaCaT) were purchased from CLS (Cell Lines Service, D69214 Eppelhein, Ger-many) and cultivated in DMEM/high glucose; 2 mM glutamine; Pen/Strep 1%; FBS 10%. Cells were dissociated using an appropriate volume of pre-warmed TrypLE™ Select cell dissociation reagent

(Sigma–Aldrich) to the flask (i.e., 1 mL in a T25 cm^2 flask). Then, complete growth medium was added and the cells were pelletted at 250g × 5 min. HaCaT cells were resuspended in medium with 10% FBS and plated 5000 cells per well in 96-well plates. After 24 h, cells were treated with compound (R,S)-**33** HCl in the concen-tration range 1×10^{-8} to 1×10^{-5} and incubated for 48 or 72 h at 37 °C, 5% CO_2 in media with 5% FBS ($N = 6$) or without serum ($N = 6$). A MTT based citotoxicity test (CellTiter 96® AQueous One Solution Cell Proliferation Assay, Promega) was performed and the optical density was read in a microplate reader (BioTek® Instruments, Inc.).

5.2.4.5. Statistical analysis. Data are expressed as the mean ± standard error of the mean (SEM). Statistical analysis was performed by two-way analysis of variance (ANOVA) and post hoc Bonferroni/Dunn test. Values of p less than 0.05 were consid-ered statistically significant.

5.3. Computational study

5.3.1. Drug-like properties

Drug-like properties such as log$P$, pK_a, and log$D$ at pH 7.4 were calculated using MARVIN.[33] For log$P$ calculations, MARVIN used a predefined pool of fragments[34] and the extended group contribu-tion approach.[35] pK_a values were calculated from empirically calculated partial charges, and hydrogen bonds were also parame-terized and taken into account within the calculation. First, MAR-VIN assigns ionization sites to the molecule. Then, it generates all microspecies and calculates partial charge distribution of micro-species. After that, it calculates the micro ionization constant pK_a for microspecies. Finally, it calculates the ratio of microspecies and macro ionization constant pK_a. From values of log$P$ and pK_a, log$D$ was determined at desired pH.

5.3.2. Pharmacophore modeling

The molecules reported in this work and the ones reported in our previous work[20] were sketched by using the SYBYL program.[36] They were optimized and their activities were collected as log(1/K_i) values. Pharmacophore modeling was achieved by using the GALAHAD method. Pharmacophore models consist of a group of features that are positioned relative to each other in coordinate space as points surrounded by a sphere of tolerance. Each sphere represents the region in space that should be occupied by a certain chemical functionality capable of the kind of interaction specified by the feature type. GALAHAD is able to identify a set of ligand con-formations that have an optimal combination of low strain energy (SE), steric overlap (SO), and pharmacophoric similarity (PhS). GAL-AHAD conducts the model building process into two stages: (1) GA search in the internal coordinates (torsional space) and (2) align-ment of the conformers produced in cartesian space by a linear assignment routine.[37] GALAHAD uses a true multi-objective (MO) function in which each term (SE, SO, and PhS) is considered inde-pendently.[38] This MO functions are employed for three different purposes: to assess reproductive fitness, to select which candidates should survive to the next generation, and to rank models after Cartesian alignment of their constituent ligand conformers. The three MO functions constitute a multi-objective triage (MOTriage) approach, which make use of the Pareto rank for each individual model.[39]

Ten of the most active σ_1 ligands were selected to generate pharmacophore models. GALAHAD was run for 100 generations with a population size of 60 and a tournament pool size of 250. De-fault values were used for other settings. Only models with more than 8 ligands with contribution to the consensus feature were considered. Between the selected models, the one with the best

SE, SO, and PhS values based on Pareto ranking was selected as the best model.

Supplementary data

Supplementary data associated with this article can be found, in the online version, at doi:10.1016/j.bmc.2011.09.016.

References and notes

1. Maurice, T.; Su, T. P. *Pharmacol. Ther.* **2009**, *124*, 195.
2. Crawford, K. W.; Bowen, W. D. *Cancer Res.* **2002**, *62*, 313.
3. Mavlyutov, T. A.; Epstein, M. L.; Andersen, K. A.; Ziskind-Conhaim, L.; Ruoho, A. E. *Neuroscience* **2010**, *167*, 247.
4. Hanner, M.; Moebius, F. F.; Flandorfer, A.; Knaus, H. G.; Striessnig, J.; Kempner, E.; Glossmann, H. *Proc. Natl. Acad. Sci. U.S.A.* **1996**, *93*, 8072.
5. Kekuda, R.; Prasad, P. D.; Fei, Y. J.; Leibach, F. H.; Ganapathy, V. *Biochem. Biophys. Res. Commun.* **1996**, *229*, 553.
6. Seth, P.; Leibach, F. H.; Ganapathy, V. *Biochem. Biophys. Res. Commun.* **1997**, *241*, 535.
7. Seth, P.; Fei, Y. J.; Li, H. W.; Huang, W.; Leibach, F. H.; Ganapathy, V. *J. Neurochem.* **1998**, *70*, 922.
8. Toussaint, M.; Debreu-Fontaine, M. A.; Maurice, T.; Melnyk, P. *Med. Chem.* **2010**, *6*, 355.
9. Hayashi, T.; Rizzuto, R.; Hajnoczky, G.; Su, T. P. *Trends Cell Biol.* **2009**, *19*, 81.
10. Su, T. P.; Hayashi, T.; Maurice, T.; Buch, S.; Ruoho, A. E. *Trends Pharmacol. Sci.* **2010**, *31*, 57.
11. Morin-Surun, M. P.; Collin, T.; Denavit-Saubie, M.; Baulieu, E. E.; Monnet, F. P. *Proc. Natl. Acad. Sci. U.S.A.* **1999**, *96*, 8196.
12. Hayashi, T.; Su, T. P. *J. Pharmacol. Exp. Ther.* **2003**, *306*, 726.
13. Hayashi, T.; Su, T. P. *Cell* **2007**, *131*, 596.
14. Meunier, J.; Hayashi, T. *J. Pharmacol. Exp. Ther.* **2010**, *332*, 388.
15. Luty, A. A.; Kwok, J. B.; Dobson-Stone, C.; Loy, C. T.; Coupland, K. G.; Karlstrom, H.; Sobow, T.; Tchorzewska, J.; Maruszak, A.; Barcikowska, M.; Panegyres, P. K.; Zekanowski, C.; Brooks, W. S.; Williams, K. L.; Blair, I. P.; Mather, K. A.; Sachdev, P. S.; Halliday, G. M.; Schofield, P. R. *Ann. Neurol.* **2010**, *68*, 639.
16. Sassone-Corsi, P.; Der, C. J.; Verma, I. M. *Mol. Cell. Biol.* **1989**, *8*, 3174.
17. Takebayashi, M.; Hayashi, T.; Su, T. P. *J. Pharmacol. Exp. Ther.* **2002**, *303*, 1227.
18. Takebayashi, M.; Hayashi, T.; Su, T. P. *Synapse* **2004**, *53*, 90.
19. Guzman-Lenis, M. S.; Navarro, X.; Casas, C. *Neuroscience* **2009**, *162*, 31.
20. Collina, S.; Loddo, G.; Urbano, M.; Linati, L.; Callegari, A.; Ortuso, F.; Alcaro, S.; Laggner, C.; Langer, T.; Prezzavento, O.; Ronsisvalle, G.; Azzolina, O. *Bioorg. Med. Chem.* **2007**, *15*, 771.
21. Rossi, D.; Urbano, M.; Pedrali, A.; Serra, M.; Zampieri, D.; Mamolo, M. G.; Laggner, C.; Zanette, C.; Florio, C.; Schepmann, D.; Wuensch, B.; Azzolina, O.; Collina, S. *Bioorg. Med. Chem.* **2010**, *18*, 1204.
22. Richmond, N. J.; Abrams, C. A.; Wolohan, P. R. N.; Abrahamian, E.; Willett, P.; Clark, R. D. *Aided Mol. Des.* **2006**, *20*, 567.
23. Lipinski, C. A.; Lombardo, F.; Dominy, B. W.; Feeney, P. J. *Adv. Drug Deliv. Rev.* **2001**, *46*, 3.
24. Caballero, J. *J. Mol. Graph. Model.* **2010**, *29*, 363.
25. Mégalizzi, V.; Mathieu, V.; Mijatovic, T.; Gailly, P.; Debeir, O.; De Neve, N.; Van Damme, M.; Bontempi, G.; Haibe-Kains, B.; Decaestecker, C.; Kondo, Y.; Kiss, R.; Lefranc, F. *Neoplasia* **2007**, *9*, 358.
26. Nishimura, T.; Ishima, T.; Iyo, M.; Hashimoto, K. *PLoS One* **2008**, *3*, e2558.
27. Ishima, T.; Nishimura, T.; Iyo, M.; Hashimoto, K. *Prog. Neuro-Psychopharmacol. Biol. Psychiatry* **2008**, *32*, 1656.
28. Tan, F.; Guio-Aguilar, P. L.; Downes, C.; Zhang, M.; O'Donovan, L.; Callaway, J. K.; Crack, P. J. *Neuropharmacology* **2010**, *59*, 416.
29. Perrin, D. D.; Armarego, W. L. F. *Purification of Laboratory Chemicals*, 3th ed.; Pergamon Press: Oxford, 1988.
30. Matsumoto, R. R.; Bowen, W. D.; Tom, M. A.; Vo, V. N.; Truong, D. D.; De Costa, B. R. *Eur. J. Pharmacol.* **1995**, *280*, 301.
31. Mach, R. H.; Smith, C. R.; Childers, S. R. *Life Sci.* **1995**, 57.
32. Bradford, M. M. *Anal. Biochem.* **1976**, *72*, 248.
33. Kashiwagi, H.; McDunn, J. E.; Simon, P. O., Jr.; Goedegebuure, P. S.; Xu, J.; Jones, L.; Chang, K.; Johnston, F.; Trinkaus, K.; Hotchkiss, R. S.; Mach, R. H.; Hawkins, W. G. *Mol. Cancer* **2007**, *6*, 48. doi:10.1186/1476-4598-6-48.
34. Kashiwagi, H.; McDunn, J. E.; Simon, P. O., Jr.; Goedegebuure, P. S.; Vangveravong, S.; Chang, K.; Hotchkiss, R. S.; Mach, R. H.; Hawkins, W. G. *J. Transl. Med.* **2009**, *7*, 24. doi:10.1186/1479-5876-7-24.
35. Azzariti, A.; Colabufo, N. A.; Berardi, F.; Porcelli, L.; Niso, M.; Simone, G. M.; Perrone, R.; Paradiso, A. *Mol. Cancer Ther.* **2006**, *5*, 1807.
36. SYBYL, version 7.3; Tripos Inc.: 1699 South Hanley Rd., St. Louis, MO 63144, USA, 2006.
37. Richmond, N. J.; Willett, P.; Clark, R. D. *J. Mol. Graph. Model.* **2004**, *23*, 199.
38. Gillet, V. J.; Khatib, W.; Willett, P.; Fleming, P. J.; Green, D. V. S. *J. Chem. Inf. Comput. Sci.* **2002**, *42*, 375.
39. Clark, R.; Abrahamian, E. *J. Comput. Aided Mol. Des.* **2009**, *23*, 765.